Weaver, P.P.E., Schmincke, H.-U., Firth, J.V., and Duffield, W. (Eds.), 1998
Proceedings of the Ocean Drilling Program, Scientific Results, Vol. 157

16. TEPHRA EVENT STRATIGRAPHY AND EMPLACEMENT OF VOLCANICLASTIC SEDIMENTS, MOGÁN AND FATAGA STRATIGRAPHIC INTERVALS, PART II: ORIGIN AND EMPLACEMENT OF VOLCANICLASTIC LAYERS[1]

Hans-Ulrich Schmincke[2] and Mari Sumita[2]

ABSTRACT

We subdivided volcaniclastic layers drilled during Leg 157 around Gran Canaria at distances up to 70 km from the shore of the island at Hole 953C, 955A, and 956B deposited between 14 and ~11.5 Ma into >100 volcaniclastic units at each site. Most volcaniclastic layers are <20 cm thick, but complex turbidite units up to 1.5 m thick make up 10% to 20% of all volcaniclastic units in Holes 953C and 956B. We distinguish several types of clasts: felsic vitroclasts, (1) bubble-wall/junction shards, (2) brown nonvesicular felsic shards, (3) welded tuff clasts, (4) pumice shards, and (5) sideromelane shards. Mineral phases comprise anorthoclase and lesser amounts of plagioclase, calcic and sodic amphibole (kaersutite, richterite, and edenite), clinopyroxene (titanaugite to aegirine), hypersthene, minor enstatite, phlogopite, Fe/Ti oxides, sphene, chevkinite, apatite, and zircon. Xenocrysts are dominantly titanaugite derived from the subaerial and submarine shield basalts. Lithoclasts are mainly tachylitic and crystalline basalt, the latter most common in Hole 953C, and fragments of felsic lava and ignimbrite. Bioclasts consist of open planktonic foraminifers and nannofossil ooze in the highly vitric layers, while filled planktonic foraminifers, benthic foraminifers, and a variety of shallow water calcareous and siliceous fossils and littoral skeletal debris are common in the basal coarser grained parts of turbidites.

Volcaniclastic sedimentation during the time interval 14–9 Ma was governed dominantly by direct and indirect volcanic processes rather than by climate and erosion. Most volcaniclastic units thought to represent ignimbrite eruptions consist of a coarse basal part in which pumice and large brown nonvesicular and welded tuff shards and crystals dominate, and an upper part that commonly consists of thin turbidites highly enriched in bubble-wall shards. The prominent coarser grained and vitroclast-rich volcaniclastic layers were probably emplaced dominantly by turbidity currents immediately following entry of ash flows into the sea. The brown, blocky and splintery, dense, completely welded, dominantly angular to subrounded, partially to completely welded tuff shards are thought to have formed by quench fragmentation (thermal shock) as the hot pyroclastic flows entered the sea, fragmentation of cooling ignimbrite sheets forming cliffs along the shore, and water vapor explosions in shallow water. Well-sorted beds dominated by bubble-wall/junction shards may have formed by significant sorting processes during turbidite transport into the deep (300–4000 m) marine basins north and south of Gran Canaria. Some may also have been generated largely by grinding of pumice rafts and fallout and/or by interface-shearing of coignimbrite ash clouds traveling over the water surface.

Generally fresh sideromelane shards that occur dispersed in many felsic volcaniclastic layers and in one hyaloclastite layer are mostly nonvesicular and blocky. They indicate submarine basaltic eruptions at water depths of several hundred meters on the slope of Gran Canaria synchronously with felsic ash flow eruptions on land. Most sideromelane shards are slightly evolved (4–6 wt% MgO), but shards in some layers are mafic (6–8 wt% MgO). Most shards have alkali basaltic compositions. The dense, iron-rich, moderately evolved basaltic magmas are thought to be the direct parent magmas for the trachytic to rhyolitic magmas of the Mogán Group. They were probably unable to erupt beneath the thick, low-density lid of the felsic magma reservoir below the large caldera but were erupted through lateral dikes onto the flanks of the submarine cone. Tholeiitic shards occur low in the stratigraphic section where peraluminous K-poor magmas were erupted, a correlation that supports the parental relationship.

Heterogeneity in glass and crystal populations in the absence of other evidence for an epiclastic origin, probably largely reflect systematic primary compositional heterogeneity of most of the ignimbrites, which become more mafic toward the top. This gross compositional zonation is destroyed at the land/sea interface, where the ignimbrites are likely to have resulted in a chaotic buildup of large, quickly cooled, and fragmented mounds of hot ignimbrite. Post-emplacement, erosional mixing is probably reflected in volcaniclastic layers that are well bedded, contain a large amount of shallow water skeletal debris and rounded basaltic lithoclast, and show a wide spectrum of glass and mineral compositions. Basaltic lithoclasts are much more common in volcaniclastic layers at Hole 953C, probably because the northeastern shield basalts were highly dissected in this older part of the composite shield volcano prior to the beginning of ignimbrite volcanism at 14 Ma. As a result, many ignimbrites may have been channeled into the sea via deep canyons. In contrast, erosion was minimal during Mogán time in the southern half of the island, which was gently sloping and practically undissected, leading to concentric sedimentation on the volcanic apron. In general, the submarine, syn-ignimbrite turbidites have preserved a number of characteristics from the pristine stage of ash flow emplacement—especially shape and vesicularity of primary particles and the transient glassy state—that are lacking in the subaerial ignimbrites that cooled and devitrified at high temperatures.

INTRODUCTION

Among intraplate oceanic islands, Gran Canaria contains unusually large volumes of felsic volcanic deposits, which resulted predominantly from explosive eruptions following the middle Miocene basaltic shield-building stage (Figs. 1–3). A condensed stratigraphic description is given in Sumita and Schmincke (Chap. 15, this volume), and ages are presented by Bogaard and Schmincke (Chap. 11,

[1]Weaver, P.P.E., Schmincke, H.-U., Firth, J.V., and Duffield, W. (Eds.), 1998. *Proc. ODP, Sci. Results*, 157: College Station, TX (Ocean Drilling Program).

[2]GEOMAR Forschungszentrum, Wischhofstrasse 1-3, D-24148 Kiel, Federal Republic of Germany. hschmincke@geomar.de

Prior Chapter Contents Next Chapter

this volume). We estimate that between 300 and 500 km^3 (dense rock equivalent: DRE) of dominantly peralkaline trachytic, comenditic, and pantelleritic magmas were erupted between ~14 and 13.3 Ma, forming the subaerial Mogán Group (Schmincke, 1994). This figure has to be roughly doubled based on the large volume of correlative submarine volcaniclastic layers drilled. During the eruptive period of the Fataga phase (chiefly ~13–9.5, lasting to ~8.5 Ma), probably >500 km^3 of dominantly trachyphonolitic magmas were erupted, a significant fraction as lava flows. In total, >1000 km^3 of felsic magma was erupted on land over a main period of 4 to 5 m.y. Almost no basalts were erupted subaerially during this time, except for a thin but widespread basalt unit (T4), which separates the Middle and the Upper Mogán Formations at ~13.6 Ma, and very local basalts in the Lower (T3) and Middle (T6) Mogán Formations. Evidence from land-based studies suggests that nearly all of the ~15 Mogán cooling units were emplaced as pyroclastic flows that spread radially from the central Tejeda caldera. Minor fallout tuffs are preserved beneath some of the ignimbrite cooling units, whereas only one low-silica rhyolite unit was emplaced as a lava flow (unit VL of the Lower Mogán Formation). The growth and destruction of Gran Canaria was thus punctuated by numerous volcanic events, including major explosive eruptions that produced large ash flows and/or ash falls, and debris avalanches. Here, we characterize the volcaniclastic deposits that resulted chiefly from entry of pyroclastic flows into the sea and attempt to interpret their origin, specifically their fragmentation and emplacement mechanisms.

Few criteria exist for distinguishing between primary volcaniclastic deposits and volcanic particles produced by erosion of pre-existing rocks. Alternating short, but highly productive, volcanic phases with longer erosional periods on Gran Canaria, as well as evidence that many of the Miocene ash flows must have entered the sea, provide an excellent opportunity to better understand how primary volcanic flows are modified and transformed into sediment mass flows at the land/sea interface.

Although four sites were drilled in the clastic apron of Gran Canaria (Fig. 1), we will not discuss Site 954 because the entire interval representing the Mogán and Fataga stratigraphy is missing at this site. Because our study of the Fataga ignimbrites on land is much less detailed than that of the Mogán ignimbrites and because individual Mogán ignimbrites almost invariably had much larger volumes than most of the Fataga ignimbrites, our conclusions are much better supported for the Mogán than for the Fataga volcaniclastic units.

SUBAERIAL DEPOSITS ON GRAN CANARIA

Ignimbrites

Volcaniclastic deposits dominate the Mogán and Fataga stratigraphic intervals on land (Figs. 1–3). They include (1) strongly welded ignimbrite cooling units, (2) unwelded to partially welded pumice flow deposits, some zeolitized, (3) agglutinates and spatter flows, (4) rare rhyolitic and common trachyphonolitic lava flows and breccias, (5) debris avalanche deposits, and (6) lahars. Some cooling units (e.g., U, VI, and TL) show structures that are intermediate between ignimbrites and classic silicic lava flows (Schmincke, 1969a, 1969b, 1974). The basal 10–20 cm of most cooling units have been welded and quenched to a compact vitrophyre, now generally altered to light buff colored clay. Rare fresh nonhydrated glass ("apache tears") occurs locally in these perlitic or thoroughly argillized vitrophyres. Fallout tephra sheets are especially widespread in the Lower Mogán Formation below cooling Units U, VL, VI, and TL above basalt-rhyolite ignimbrites P1 and R. The fallout tephra layers below VL and VI are indistinguishable by their phenocryst mineralogy, as are the lava flow VL and ignimbrite VI. Both are thought to have been erupted within a very short time span, perhaps at most a few thousand years. Fallout tephras were more widespread initially and were largely removed by wind or incorporated into the ash flows emplaced soon after the fallout sheets.

Felsic Lava Flows

The first major cooling unit on land above ignimbrite R (Fig. 3) is a widespread thick lava flow (VL) that occurs between Barrancos de Veneguera and Tasartico in the south-southwest and in Barranco de Tirajana in the southeast. This flow is much less widespread than the Mogán ignimbrites but is far thicker, locally exceeding 100 m as in Barrancos Veneguera and Tirajana.

Epiclastic Volcaniclastic Rocks

Nonvolcanic intervals are much more common in the Fataga Group as compared with the Mogán, as shown by the much larger age gaps between units (Bogaard and Schmincke, Chap. 11, this volume) and the abundance of epiclastic sediments, conglomerates, lahars, and erosional canyon-cutting between individual Fataga cooling units. Within the Fataga stratigraphic interval, we have recognized three major intervals of debris-avalanche/debris-flow units. The debris-flow deposits are up to several meters thick and are characterized by the occurrence of lenses up to several meters in diameter of matrix-free shattered rock interpreted to have formed from debris avalanches.

DESCRIPTION OF VOLCANICLASTIC LAYERS IN THE CORES

Here we focus on the Mogán and Lower Fataga stratigraphic intervals, which cover the time period between ~14 and 12 Ma, because volcanic activity during this time was most intense and the relative proportion of volcanic sediments in the cores is highest.

Our main purpose is to develop criteria to distinguish volcaniclastic layers directly related to an ash flow or explosive eruption generating fallout ash layers and volcanic debris flows from those resulting entirely from erosion and/or redeposition from previously deposited cooled volcanic rocks. In other words we will provide criteria to show that many turbidite deposits that formed almost synchronously with entry of pyroclastic flows into the sea are in a sense hybrid and are here viewed generously as pyroclastic to distinguish them from those formed much later by erosion of the cooled deposit. We realize that no clearcut distinction can be made.

Definition of Clasts

We have distinguished four major groups of clasts in the volcaniclastic units: vitroclasts, crystals, lithoclasts, and bioclasts.

Vitroclasts

We distinguish several major types of felsic glass and basaltic glass (sideromelane; Pls. 1–5).

Felsic Bubble-Wall and Bubble-Junction (Tricuspate) Shards

The most common type of felsic glass shard consists of fragments of vesicular pumice. These shards range from silt size to 0.5 mm. Glass shards in pure or nearly pure vitric tuffs are generally < 0.2 mm in diameter. Glass septa in the shards tend to be thicker in the rhyolitic/trachytic Mogán ashes than in those of the trachyphonolitic Fataga formations (Pl. 4, Figs. 1–6).

Globular Shards

Some vitric tuffs are dominated by globular shards (Pl. 4, fig. 3) that are characteristic of the unwelded zones of low viscosity peral-

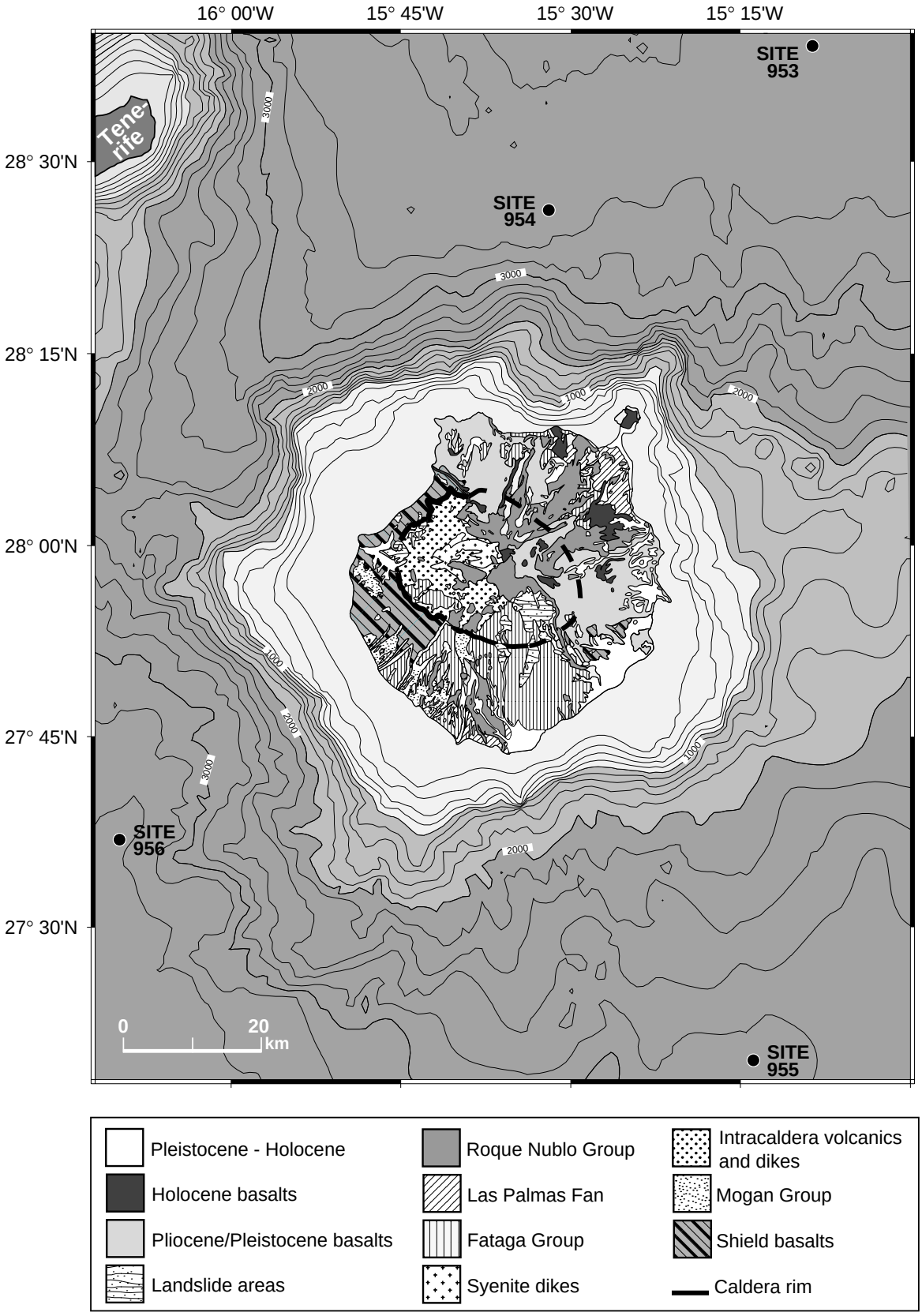

Figure 1. Simplified geology and bathymetry of Gran Canaria. Bathymetry after Funck and Schmincke (in press).

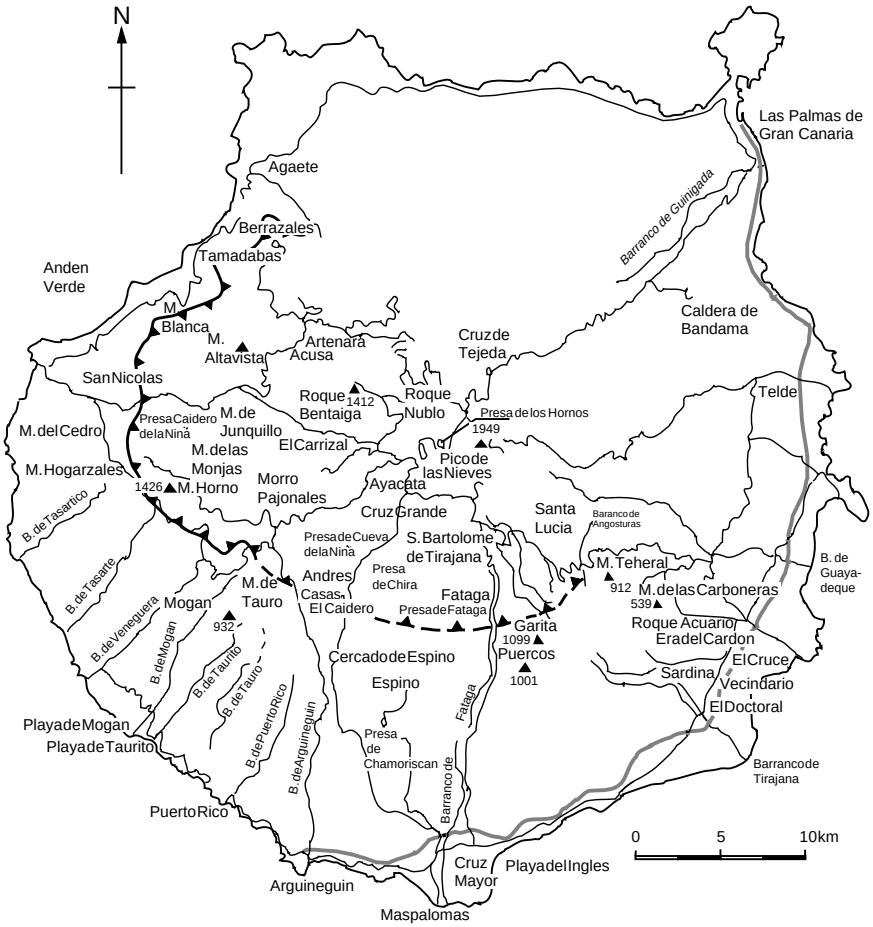

Figure 2. Major canyon systems and localities on Gran Canaria mentioned in the text.

kaline ignimbrites (Schmincke, 1974). They are generally brown, reflecting slower cooling compared to the dominantly colorless bubble-wall shards.

Pumice Shards

Pumice shards range in size from small lapilli (<2 cm) to fine ash (0.1 mm). They are the dominant shard type in some units (Figs. 4, 5) but are generally subordinate to bubble-wall/junction shards. In bedded volcaniclastic units they are concentrated in thin laminae alternating with more crystal-rich layers. Pumice shards range from highly vesiculated to those with deformed vesicles that are interpreted as partly welded pumices (Pl. 1, Figs. 5, 6; Pl. 2; Sumita and Schmincke, Chap. 15, this volume). Tubular pumice shards are common in some volcaniclastic units. In some coarser grained tuffs and lapillistones that consist largely of pumice, flattening of vesicles is interpreted to have occurred in the cold state by compaction during and after diagenetic alteration of the glass to smectite.

Blocky Felsic Shards

A characteristic but, to our knowledge, not previously described type of glass shard is angular, nonvesicular, and brown and can be up to 5 mm in diameter (Pl. 1, Figs. 1–6; Pl. 3, Figs. 1–6; Fig. 6). Such shards occur in up to 20 or more volcaniclastic units at each site and are the dominant type of shards in some, although they are on the whole subordinate in number to bubble-wall/junction shards.

Most of the nonvesicular, blocky, felsic glass fragments are elongated and platy (Pl. 1, Figs. 1, 2; Pl. 2, Fig. 2; Pl. 3, Figs. 5, 6) resembling the splinter-like spalling shards common in hyaloclastites. Very subtle remnant, palimpsest shard outlines have been recognized in several of these glass fragments (Pl. 1, Fig. 2), indicating that they represent, probably without exception, completely welded shards. These shards are almost invariably light brown, contrasting with the generally colorless plate-like shards.

Partially Welded Tuff Clasts

Several coarse, vitric tuffs and lapillistones contain rounded clasts that are composed of clearly visible shards which are welded to various degrees (Pl. 1, Figs. 3–6). Because welding of shards in some clasts is not complete, they are likely to have been derived from the upper half or the distal margins of an ignimbrite cooling unit that had entered the sea where lower load pressure prevented more thorough welding. We speculate that these partially welded tuffs represent material from the voluminous hot ash flow deposits that are likely to have accumulated at the shore line where the ignimbrites entered the sea. Such material is not preserved on land, because the glass shards in the less strongly welded upper thirds of ignimbrite cooling units devitrified and became cemented by vapor phase crystals during slow cooling.

Sideromelane

Pale yellow shards of basaltic composition occur in many felsic volcaniclastic layers. Vesicularity in sideromelane shards is difficult to quantify. We here use a very rough subdivision into three types: (1) blocky, angular dense shards with up to 10 vol% vesicles (Pl. 5, Figs. 1, 3, 4), (2) moderately vesicular shards with 10 to 60 vol% vesicles (Pl. 5, Fig. 2), and (3) highly vesicular shards with >60 vol% vesicles. Using this classification, the sideromelane shards in the volcaniclastic units at all three sites are dominantly dense to moderately vesicu-

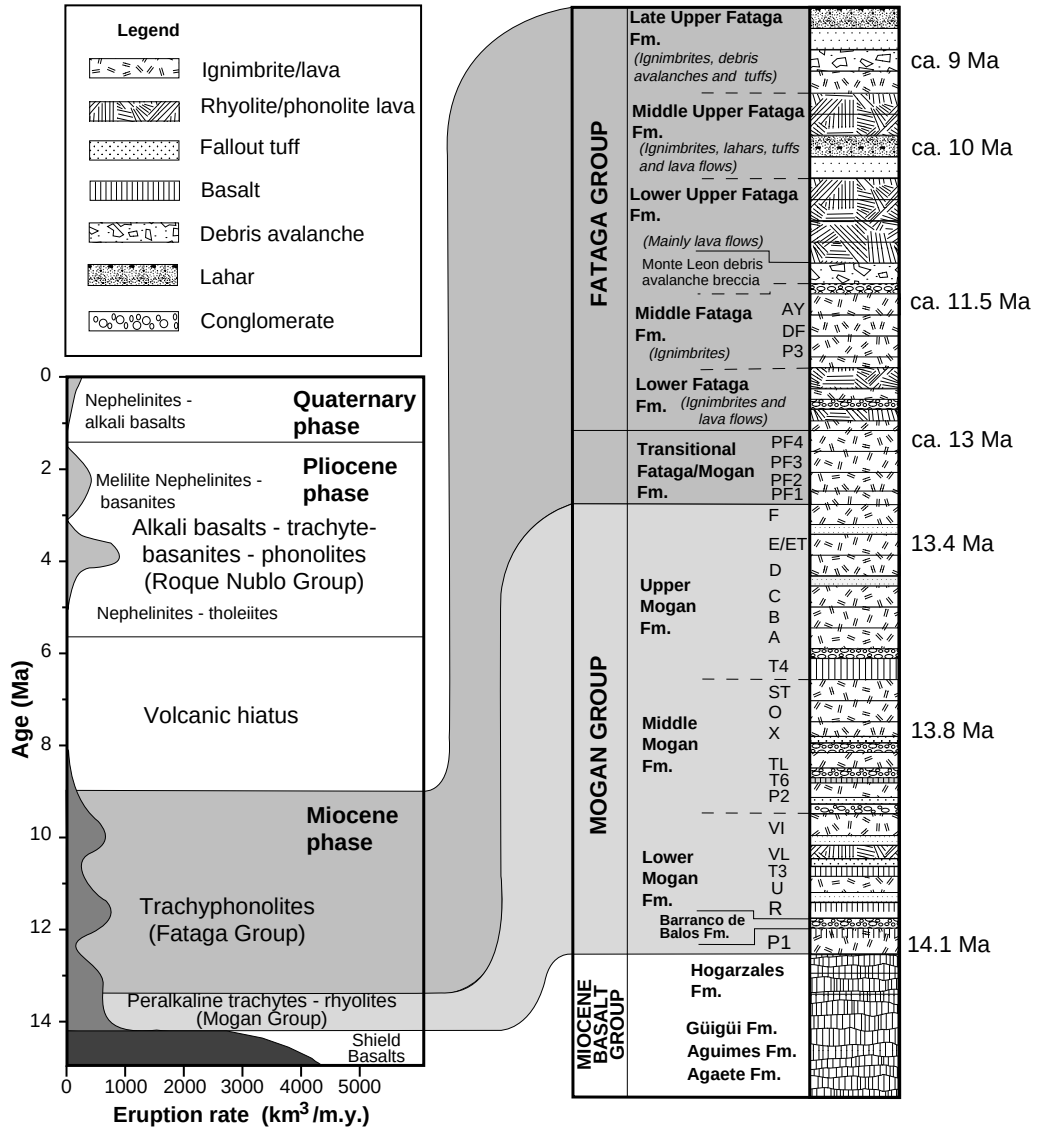

Figure 3. Stratigraphy of the main volcanic phases on Gran Canaria and detailed stratigraphy of Mogán and Fataga Formations (modified from Schmincke, 1976, 1994).

lar with generally <30 vol% vesicles. Sideromelane shards with >60 vol% vesicles, such as occur most pronounced in the hyaloclastites in the upper 15 m of lithologic Unit V (Hole 956B) and also in lithologic Unit VI and in some layers of Unit V at Hole 953C, are almost completely absent, suggesting that all basaltic eruptions generating the sideromelane shards took place at water depths greater than ~500 m. Exceptions comprise the lowermost felsic volcaniclastic units such as P1-equivalent tuffs in Hole 956B (Freundt and Schmincke, Chap. 14, this volume) where abundant extremely vesicular basaltic shards were picked up during submarine transport possibly by laterally eroding shallow water hyaloclastite tuff cones formed at the end of basaltic shield volcano activity. Theoretically such shards could also be related to quench fragmentation in the shore zone where lava flows enter the sea. Such an origin is not likely for the deposits discussed here because of the near absence of basaltic flows on land and the absence of clasts with sideromelane-tachylite textural transitions.

We define hyaloclastites as deposits consisting entirely or dominantly of glassy or formerly glassy, vesicular or nonvesicular sideromelane shards (Pl. 5; Fig. 2). We found one volcaniclastic layer (Hole 956B) consisting of 95 vol% of largely fresh, angular, light-yellow sideromelane shards with 5 vol% clinopyroxene, plagioclase, and titanomagnetite phenocrysts. The layer is 5 cm thick, but its contacts with over- and underlying sediments are not depositional, suggesting this to be a minimum thickness with an unknown amount having been lost during drilling. The grain size of the sideromelane shards ranges from 0.1 to 0.3 mm.

Crystals

Crystals occur in most volcaniclastic units and make up almost 50% by volume in a few. They are, however, essentially absent from many nearly pure fine-grained vitric tuffs. The types and composition of the main phenocryst and free mineral phases are documented in the companion paper (Sumita and Schmincke, Chap. 15, this volume).

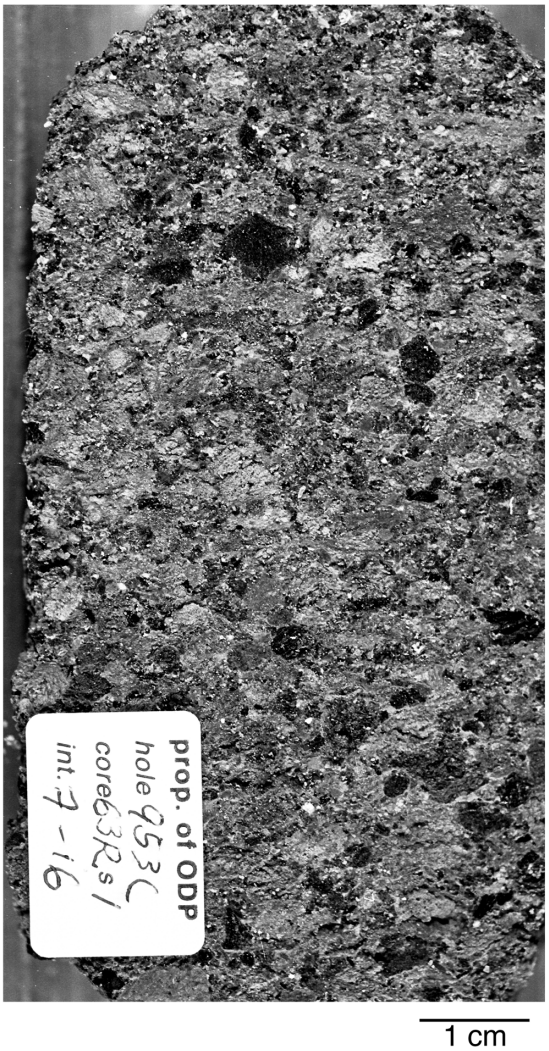

Figure 4. Pumice-rich lapillistone from the base of VU-38, interval 157-953C-63R-1, 7–16 cm.

Figure 5. Pumice (up to 3 cm in diameter) and angular glass, shard-rich lapillistone to coarse tuff, containing pick-up clasts (up to 5 cm in length) of pelagic sediment. Base of VU-43 interval 157-953C-60R-1, 0–22 cm.

Crystals range in size from 0.1 to 0.5 mm, with mafic crystals usually being smaller than the dominant anorthoclase crystals. The form of the crystals ranges from nearly euhedral in the syn-ignimbritic volcaniclastic units directly related to an eruption to subrounded in volcaniclastic layers consisting dominantly of epiclastic particles. Glomerocrysts are still intact in some volcaniclastic layers interpreted as pyroclastic fall deposits.

Lithoclasts

Basaltic Lithoclasts

The most common type of lithoclast or rock fragment is of basaltic composition and occurs in three main types.

Tachylite. The most common basaltic lithoclast is a quickly cooled, opaque tachylite, which is usually nonvesicular to very slightly vesicular. Tachylites with minor plagioclase microlites, such as those in the upper 50 m of the basaltic shield volcaniclastics in Hole 953C (lithologic Unit V) and in the upper ~10 m in Hole 956B (Schmincke and Segschneider, Chap. 12, this volume) are interpreted to be derived from basaltic lava flows and scoria cones of the subaerial shield phase. Tachylite clasts thought to have been derived from the composite rhyolite/basalt ignimbrite (P1), or the basaltic member (R) of T4 (Pl. 5, Fig. 5) are rounded, slightly vesicular, devoid of plagioclase microlites, and are discussed in more detail by Freundt and Schmincke (Chap. 14, this volume).

Crystalline Basalt. Fine-grained, fully crystallized basaltic clasts are less abundant than the tachylite fragments but may constitute up to 50 vol% of the basaltic lithoclasts in some volcaniclastic layers. These crystallized basalt fragments are almost invariably more rounded than the tachylite and are well rounded in a few layers. The occurrence of these clasts is one of the best criteria for characterizing epiclastic constituents formed by erosional abrasion on land (Schmincke and von Rad, 1979), because tachylite clasts can be primary or can represent the less quickly quenched fragments when basaltic lava enters the sea.

Altered Hyaloclastite. Small hyaloclastite fragments composed of vesicular or blocky sideromelane shards, invariably completely altered to smectite, occur as accessory lithoclasts, generally <1 vol% in several volcaniclastic layers (Pl. 5, Fig. 6). They are interpreted to

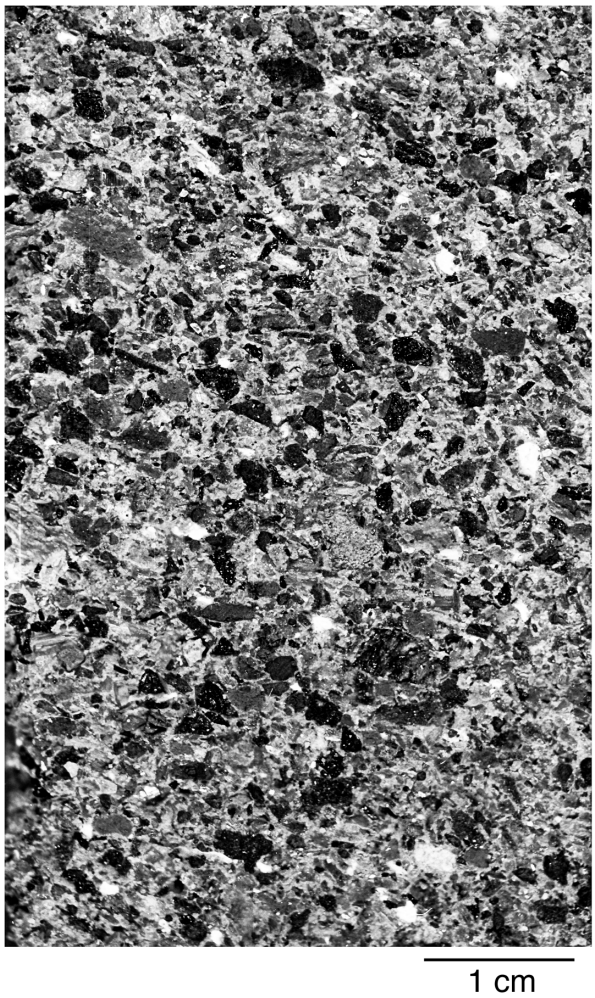

Figure 6. Coarse tuff/lapillistone rich in black angular fragments of welded glass formed by thermal cracking of hot ignimbrite that entered the sea, Hole 953C (VU-37 interval 157-953C-64R-1, 83–91 cm).

have been derived from the submarine hyaloclastite carapace (Schmincke and Segschneider, Chap. 12, this volume).

Felsic Lava Fragments

Minor amounts of felsic lava fragments occur as accessory components in many volcaniclastic layers of the Mogán Group. Some, believed to represent the quench products of rhyolite lava flow VL, are microcrystalline without showing alignment of feldspar microlites characteristic of the groundmass of the onland flow. Tentatively, we interpret this texture as quench crystallization of the hot lava flow that entered the sea and as exposed in cliffs in its hot state to wave action generating abundant fragments by quench fragmentation. The paucity of such fragments in the Mogán-equivalent volcaniclastic layers was expected because only one extra-caldera lava flow (VL) has been recognized in the Mogán Formation, whereas lava flows are more common in the intra-caldera fill. Felsic rock fragments of trachyphonolitic composition consisting dominantly of strongly aligned feldspar microlites (trachytic texture) and typically containing groundmass aegirine are more abundant in epiclastic turbidites throughout the Fataga Group volcaniclastic layers. The greater abundance of trachyphonolitic lithoclasts corresponds to the much greater volume of lava flows in the Lower and especially the Upper Fataga Formations.

Plutonic Rocks

Fragments of plutonic rocks occur in many coarser grained tuffs and lapillistones. They are dominantly syenites, composed mainly of varying amounts of alkali feldspar, clinopyroxene, and alkali amphibole or, in the Fataga stratigraphic interval, of phlogopite. Syenitic xenoliths also occur in many subaerial ignimbrites. Gabbros are rare.

Bioclasts

We distinguish planktonic and benthic foraminifers. Planktonic fossils are chiefly *Globigerina,* diatoms, and nannofossil plankton. The planktonic foraminifers occur as both unfilled chambers, which are dominantly associated with vitric tuffs, pumice tuffs and lapillistones, and foraminifers filled with dark clay, which occur together with fragments of other benthic organisms (Pl. 5, Figs. 3, 5). Among the benthic skeletal fragments, we distinguish benthic foraminifers, rotaliide foraminifers, coralline algae, echinoderms, bryozoa corals, bivalve shell fragments, amphistegina, and sponge spicules.

We have lumped all microscopic skeletal biogenic material into the bioclast category whether or not it is fragmented. We have made an effort to distinguish open planktonic foraminifers (*Globigerina*) from other bioclasts because of their importance for interpreting the transport mechanism of the volcaniclastic layers. Most common are foraminifers. Large thick shell fragments believed to have been derived from shallow-water, nearshore biota are common in the basal coarser-grained parts of syn-ignimbrite tuffs and in turbidites consisting dominantly of epiclasts. Sponge spicules are abundant in some volcaniclastic layers, especially in those at Hole 953C.

Matrix

The most common type of matrix consists of clay-size nannofossils completely re-crystallized in many volcaniclastic layers. The amount of nonbiogenic clay is difficult to estimate, but it is dominant in a few fine-grained vitric turbidites forming the top part of syn-ignimbrtite depositional units. Clay is also common in mudstones, especially in the Fataga stratigraphic interval, as also reflected in the brown color of the layers. The degree of admixture of very fine silt- to clay-size glass shards to the matrix is difficult to estimate, but thin sections of several nannofossil ooze sediments contain minor microscopically visible glass shards and we suspect a larger proportion has been dissolved.

SEDIMENTOLOGICAL FEATURES OF THE VOLCANICLASTIC UNITS

Thickness of Deposits

Volcaniclastic layers are unusually thick, with 50% of all layers being thicker than 35 cm at Hole 953C, thicker than 10 cm at Hole 956B, and thicker than 7.5 cm at Hole 955A (Figs. 1–8). Apparently, the sedimentation mechanisms were relatively constant through the Mogán and Fataga intervals because the thickness distribution is approximately constant. The much larger average thickness of volcaniclastic layers at Hole 953C (Fig. 7) is maintained through time as is the relatively small thickness at Hole 955A.

Sorting

Sorting of the volcaniclastic deposits varies widely. Most vitric shard tuffs and some volcanic sandstones are well sorted and some are devoid of matrix. Many of the heterogeneous volcaniclastic units that contain glass shards, pumice, and crystals are also well- to medium-sorted. Poorly sorted deposits are generally dominated by epiclasts and are more common in the stratigraphic intervals corresponding to the Middle and Upper Fataga Formations.

The grain size of most volcaniclastic layers is fine to medium sand (0.1–1 mm), but in some deposits coarse ash extends into the lapilli sizes. Grain diameters >5 mm are rare, except in debris-flow deposits in the Upper Fataga stratigraphic intervals at Holes 953C and 956B.

Structures

Structures of the volcaniclastic layers vary widely. We distinguish several structural types.

Thicker Volcaniclastic Depositional Units (Several cm to >1 m Thick)

Most abundant by volume and most unusual are massive, normally graded units with normal density grading—crystals concentrated near the base, pumice and small glass shards near the top. Such massive units include those dominated by crystals and glass shards and those in which pumice is the major component (Figs. 4–6). Many grade into fine-grained, massive to bedded and cross-bedded ash at the top, which may be diffuse because of intense burrowing by bottom-dwelling organisms. Especially common are thin, fine-grained vitric turbidites that form up to 10 thin, slightly normally graded beds, well sorted or clay-matrix rich, and each a few centimeters thick. These overlie the more massive graded basal parts with which they form depositional units, because of the absence of nonvolcanic sediments or burrowing between the layers. These complex depositional units are believed to be related chiefly to the entry of ignimbrites into the sea. Many of these units in cores with good recovery at Hole 953C are from 0.5 to 1.5 m thick (Fig. 7). Similar units in the same stratigraphic intervals at Holes 955A and 956B are rarely thicker than 0.5 m.

Homogeneous Volcaniclastic Units

A second type of volcaniclastic unit is homogeneous in grain size and consists dominantly of fine- to medium-grained glass shards. These are especially common at Hole 953C in the Lower Mogán stratigraphic interval and, more rarely, at the other sites and higher in the stratigraphy. They range from massive, poorly graded, and commonly slumped to units composed of a multitude of thin, graded turbidite layers mostly a few cm thick that have been deposited rapidly one after the other (Fig. 9). Such fine-grained, thick vitric volcaniclastic units are interpreted to be related to ignimbrite eruptions but which have traveled beyond the coarser grained part described above. Some may represent tephra-fall eruptions or grinding of pumice rafts.

Massive Volcaniclastic Units

The third group of thick, dominantly massive sand- to lapilli-sized deposits consists of well- to medium-sorted pumice and chiefly lithic components. These deposits, characteristic of the Upper Fataga interval in Hole 956B (black units in Cores 157-956B-32R through 35R) and more rarely at the other three holes, are distinguished from the other two groups by a lack of fine-grained ash in the matrix or in their upper parts and by being only weakly to nongraded with sharp lower and upper boundaries. They are interpreted as epiclastic grain-flow deposits, as reflected in their polymict lithoclast composition. Many are entirely basaltic (Core 157-956B-32R), others mixed phonolitic-basaltic.

Bedded Deposits

Finely laminated to well-bedded and cross-bedded volcaniclastic units are most common at the base of nonvolcanic turbidite beds. They are generally only a few millimeters to a few centimeters thick, but we suspect drilling loss is most severe in these layers because most are poorly consolidated.

DISCUSSION

Felsic Volcaniclastic Layers

Volcaniclastic Layers Directly Related to Ash Flow Eruptions on Land

One of our primary goals was to find out whether the common thick volcaniclastic layers are directly related to volcanic eruptions or whether rapidly erupted pyroclastic material first accumulated on the slopes of the island until it became reworked and was transported into the depositional basin by submarine mass flow, possibly via shallow marine intermediate depositional centers. Processes that occur during entry of pyroclastic flows into the sea have been the subject of lively debate for the last 15 yr. The literature up to the late 1980s is reviewed in Fisher and Schmincke (1984) and Cas and Wright (1987), and more recently by Orton (1991) and Cas and Wright (1991).

This first-order correlation between submarine tephra layers and the potential subaerial source volcanic eruption can be further subdivided into (1) deposition during the eruption, allowing for transport

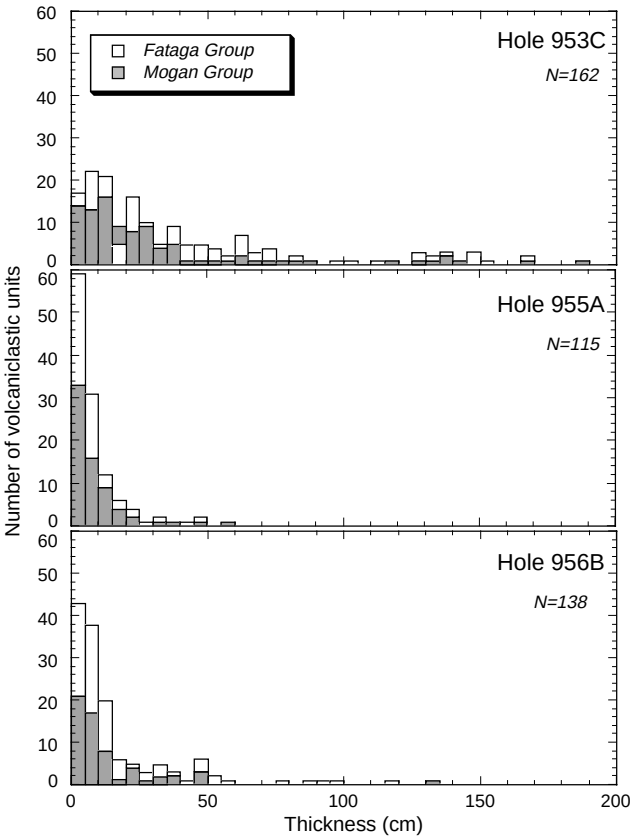

Figure 7. Thickness distribution of volcaniclastic units at Holes 953C, 955A, and 956B.

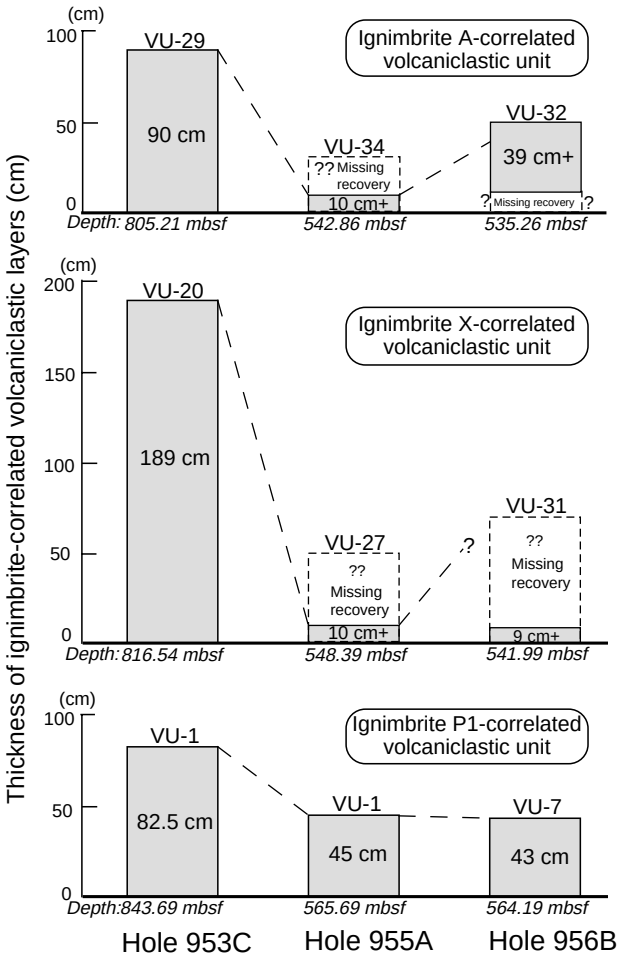

Figure 8. Comparison of recovered and "reconstructed" thicknesses of characteristic Mogán volcaniclastic units correlated with subaerial tuffs P1, X, and A at all three drill sites, emphasizing the large thickness of volcaniclastic units at Hole 953C, which is the most distant from Gran Canaria.

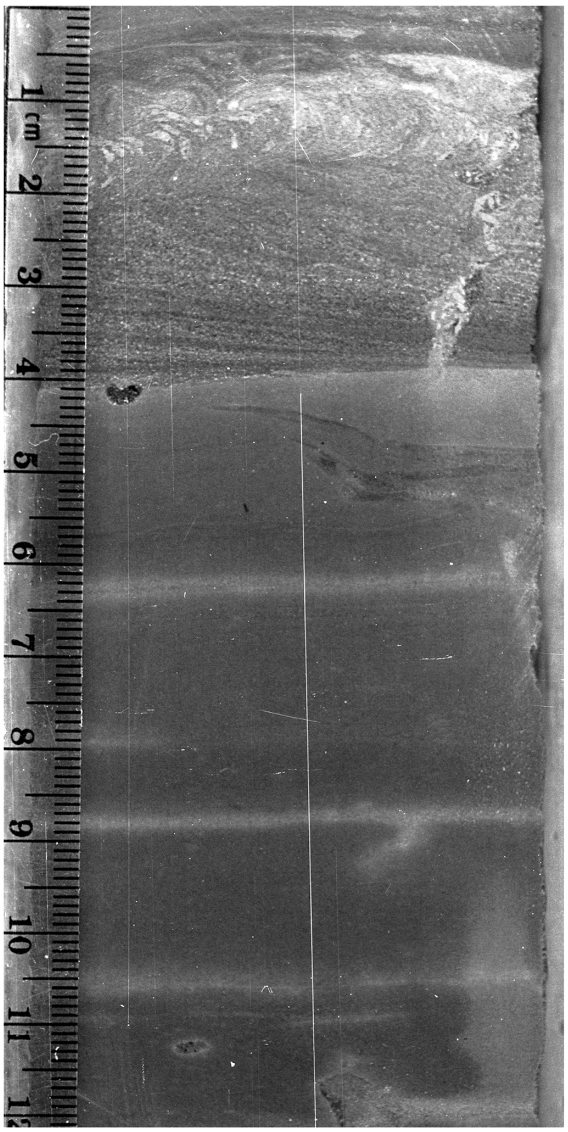

Figure 9. Thin fine-grained vitric tuff turbidites overlying medium-grained

from land or air to the final depositional sites, and (2) rapid sheetwash on land and subsequent transfer into the sedimentary basin in the aftermath of an eruption (Fig. 10). Many subaerial explosive eruptions on land are followed by major sediment mass transport over several months to years, owing to more or less complete destruction of vegetation and the existing drainage system, and deposition of many meters of unconsolidated ash. Conceivably, the large amounts of loose ash transported to the deep sea following an eruption might be very difficult to distinguish from those volcaniclastic layers that are deposited directly following an eruption.

Submarine volcaniclastic layers directly related to an eruption can be theoretically subdivided into (1) fallout layers preceding and/or following an ash flow eruption, (2) co-ignimbrite tephra layers generated above a moving pyroclastic flow, becoming airborne prior to settling into the sea or continuing as a laterally moving ground-hugging ash cloud, (3) shearing at the interface of an inflated pyroclastic flow (ash cloud) as it travels over the water surface, (4) production of shards by grinding of pumice rafts that may have a lifetime of several years following an eruption and (5) mixing of a pyroclastic flow with water as it enters the sea and continues as mass-flow downslope (Fig. 10). We must, of course, also consider the possibility that volcaniclastic layers, interpreted as having been emplaced by mass flow based on textural and structural criteria, could have been related to a fallout event during which ashes passively settled in shallow water and subsequently became remobilized and transported to the deep sea by submarine gravity flow.

We use several criteria to identify volcaniclastic layers related to ash flows entering the sea. If an ash layer is identical to a characteristic ignimbrite on land in stratigraphic position, age, glass chemistry, and phenocryst mineralogy, we are confident that it was deposited practically synchronously with the ignimbrite. The volcanic units that we believe directly represent transformation of pyroclastic flows into turbidites include most of the units already correlated unequivocally within the Mogán interval using a variety of compositional criteria (Sumita and Schmincke, Chap. 15, this volume). These include ignimbrite P1 (Freundt and Schmincke, Chap. 14, this volume), and ignimbrites VI, X, O, A, B, C, and D. As our work continues, we suspect to be able to at least double this number. The volcaniclastic units interpreted to have formed by turbidites as a direct result of the entry of pyroclastic flows into the sea are characterized by all or most of the following parameters: (1) exact correlation between source ignimbrite and syn-ignimbrite tephra layers in mineralogy and/or chemistry, (2) unusual thickness, in some cases exceeding 50 cm, (3) abun-

dant pumice lapilli, (4) occurrence or abundance of blocky, angular, nonvesicular brown glass fragments, some showing evidence of having formed by complete welding of glass shards, (5) occurrence of fragments of welded tuff, (6) little or no mixing with nonvolcanic components, mostly foraminifers, (7) moderate sorting, (8) lack of rounding of clasts, and (9) compositional spectra in the glass and/or mineral compositions that reflect the fact that all ignimbrites on Gran Canaria studied in detail are compositionally zoned and mixed. No single criterion listed above is by itself diagnostic, so that most criteria must be fulfilled to substantiate this interpretation.

Fallout Tephra Layers

We have attempted to distinguish between products of fallout, independent of whether it occurred prior to or after ignimbrite eruption, from either an airborne column over the vent or co-ignimbrite ash cloud and volcaniclastic layers transported by mass flow. We interpret volcaniclastic layers to be the result from fallout using all or most of several diagnostic criteria: (1) good to excellent sorting, (2) nonerosional base, (3) absence or paucity of pumice, crystals, lithic clasts and bioclasts, matrix, and nonvesicular blocky glass shards, (4) small thickness (generally smaller than 10 cm), (5) angular shape of shards, (6) compositional homogeneity, and (7) small grain size of shards. We have provisionally identified about five volcaniclastic units in each site as fallout tephra layers.

Most fallout tephra layers contain only minor (generally <1 vol%) small crystal fragments of one diagnostic mineral assemblage. A few layers do not follow this latter criterion, because they are composed of >95% crystals. An excellent example is volcaniclastic Unit 19 (interval 157-956B-42R-1, 87–88 cm), which is 2 cm thick and consists of a nonbedded crystal tuff composed entirely of feldspar, clino- and orthopyroxene, and magnetite with minor ilmenite and zircon and traces of sphene. The mafic crystals occur in unusually large amounts and glomerocrysts are completely unbroken. Most likely, these crystals were concentrated largely during sedimentation in the water column >3000 m deep while the more slowly settling associated glass shards were carried away by currents. Judging from modal analyses of many ignimbrites and lava flows on land, the source magma during eruption contained at most 10 vol% and more likely <5 vol% phenocrysts. This indicates an extreme crystal enrichment during eolian transport and probably most effectively submarine sedimentation. The lithostratigraphic interval above ignimbrites P1 and R in the Lower Mogán, in which this crystal tuff occurs, is also represented at all three sites by thick, fine-grained, light-brown ash turbidites that form unusually homogeneous and well-sorted deposits. Some of these volcaniclastic layers are interpreted as fallout related to lava flow VL and ignimbrite VI and their associated fallout tuffs. They have thicknesses equal to or even greater (Hole 956B) than those on land, probably because of slumping and transformation into glass shard turbidites resulting from the instability of rapidly accumulated

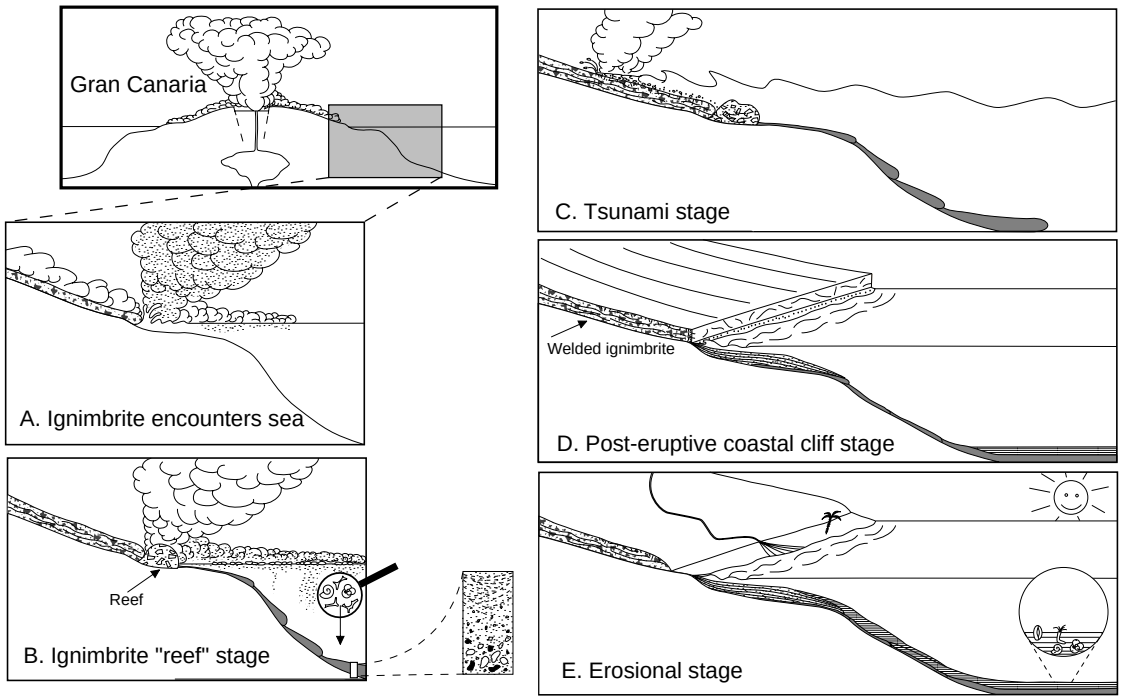

Figure 10. Sketch illustrating processes during entry of hot dense pyroclastic flows into the sea. **A.** The encounter of ash flows with the sea may involve continuation of the flow for an unknown distance under water, steam explosions, fragmentation of the upper part of pyroclastic flows, and tsunamis generated by the pyroclastic flow. **B.** Regardless of the distance, single flows may have continued under water. Interaction of seawater with a succession of flow units generates a fringe of chaotic mounds in the shore zone peripheral to the island consisting of jumbled masses of partially welded, quenched hot ash-flow material that is constantly disrupted by quench fragmentation and steam explosions. The large supply of fragmented glass generates turbidity currents that moved down the flanks of the seamount and deposited in the depositional basin. The coarse-grained turbidite deposits grade upward into finer grained tuffs consisting dominantly of bubble-wall shards that may have been generated by both shearing at the interface of co-ignimbrite ash clouds advancing over the water and by the grinding of pumice in large pumice rafts believed to result from the entry of the pyroclastic flows into the sea. **C.** Fragmentation of the surface of the freshly deposited ignimbrites is likely to occur as well as reaction to reflected waves generated by the tsunamis during entry of the voluminous flow into the sea. Material so generated is washed back to the sea by the retreating wave. **D.** A third process of fragmentation is thought to occur along the freshly exposed hot, still glassy interior of ignimbrite cooling units along the coast. Fossils in fine-grained vitric tuffs resulting from fallout through the water column are dominantly unfilled planktonic foraminifers. **E.** Volcaniclastic deposits generated during erosion of the cooled and consolidated ignimbrite in between pyroclastic flow eruptions are more heterogeneous with respect to glass and mineral composition and generally contain a broad spectrum of skeletal debris of shallow-water organisms.

thick volcaniclastic piles and the high pore pressure that must have developed inside these.

Reworked Volcaniclastic Units

Homogeneity vs. Heterogeneity

Sumita and Schmincke (Chap. 15, this volume) found glass compositions to be extremely homogeneous in some volcaniclastic units and not in others. We believe these differences can be explained in several ways.

1. Heterogeneous glass populations are simply the result of erosion of two or more ignimbrites that differ in composition. The degree of heterogeneity should increase in those stratigraphic intervals where adjacent ignimbrites differ significantly in composition, such as the Middle and Upper Mogán formations and the transition to the Fataga Formations.

2. Degree of heterogeneity should increase with time, because more ignimbrites become available for erosion and thus mixing of glass populations. Indeed, the glass shards from the Lower Mogán Formation (V-type tephra layers) are the most homogeneous compositionally.

3. Heterogeneity should be higher in volcaniclastic layers formed by erosion. Indeed, those volcaniclastics thought to be erosional based on mineral and lithoclast assemblages also contain the compositionally most diverse glass shards.

4. The heterogeneity that is petrologically most important but also most difficult to identify is that resulting from eruption of chemically diverse magmas. All ignimbrites of the Mogán Group and also those few from the Fataga Formation that we have studied in detail are compositionally zoned. In general, however, the more evolved compositions dominate in a cooling unit, with <10 vol% of an ignimbrite being more mafic.

5. Different eruptive and transport modes may also produce different extents of heterogeneity. Fallout tephra layers believed to have been deposited almost instantaneously should be more homogeneous than deposits produced by turbidity currents.

6. The final factor influencing the compositional spectrum of volcaniclastic units is the degree of alteration. Indeed, the sum total and differences in the concentrations of the two alkali elements, the most alteration-sensitive major elements in these rocks, differ appreciably from each other in most samples, even in those which show an extreme degree of homogeneity.

Although all of the above factors must have played some role in producing heterogeneity in the volcaniclastic units, we believe the three most important factors are, in decreasing order of importance: (1) epiclastic, post-emplacement erosional origin vs. synchronous deposition, (2) the dependence on stratigraphic position, and (3) different transport mechanisms for volcaniclastic units directly related to an eruption.

Criteria for Reworking

Erosion immediately following eruption should result in volcaniclastic layers that are compositionally indistinguishable from the ignimbrites. Volcaniclastic layers resulting from later erosion following cooling of a hot ignimbrite and fast removal of loose ash, and deposited prior to the next eruption, perhaps 50 k.y. later—the average time interval between Mogán ignimbrite eruptions on Gran Canaria (Bogaard and Schmincke, Chap. 11, this volume)—should contain increasingly rounded clasts and heterogeneous types and composition of particles, depending on the length of the eruption hiatus and the extent of erosion. At Holes 955A and 956B, south of the island, such heterogeneity is minimal because apparently there was little erosional dissection of ignimbrites between eruptions. Heterogeneity is more pronounced at the northeastern Site 953 owing to the more dissected subaerial terrain, which probably did not allow complete coverage of the basaltic flanks of the island by any specific ignimbrite.

The following criteria have been used to identify tuffs resulting from post-eruption reworking: (1) rounding and/or weathering of clasts, (2) compositional heterogeneity of felsic clasts, (3) admixture of older rocks, principally tachylitic and crystalline basalt, (4) variable but generally high proportion of biogenic clasts, (5) broad spectrum of biogenic fragments especially shell and coral (lithotamnia) fragments from the near-shore environment, (6) occurrence of sandy base to otherwise nonvolcanic turbidites, and (7) abundance of matrix.

For the present purpose, we simply distinguish two types of reworked volcaniclastic deposits: (1) those characterized by a high degree of compositional homogeneity and similarity to the source volcaniclastic unit, which we think record reworking immediately following an eruption, and (2) those recording erosion of the preceding deposit and older rocks in the interval between distinct volcanic events. Reworked volcaniclastic deposits of the latter type closely reflect nonvolcanic periods between major volcanic events or groups of volcanic events closely following each other.

Examples of Reworking

The relative proportions of syn-ignimbrite vs. post-eruptive volcaniclastic deposits can be judged from the nature of volcaniclastic layers in Cores 157-956B-41R through 43R. Tephra related to ignimbrite P1 makes up ~35 cm from the top of Section 157-956B-43R-3 to the lower third of 43R-2. Reworked material makes up ~30 cm in the upper part of Section 43R-2 and very thin volcaniclastic layers in most of 43R-1 (see also Freundt and Schmincke, Chap. 14, this volume). This is reasonably representative because of the good recovery in this core. Compositional Type V (no amphibole phenocrysts) begins at 7.5 cm in Section 157-956B-43R-1, and similar, generally very clean tuffs occur in three major units in Core 157-956B-42R and minor units in 41R. The total thickness in 42R of which ~35 cm was recovered is ~75 cm, whereas reworked material is probably <15 cm. Although we cannot estimate the total amount and relative proportions of primary and reworked volcaniclastic in the nonrecovered interval, the very friable nature of the primary tephra layers suggests that the nonrecovered material may have been largely primary. Similar rough calculations throughout Cores 157-956B-40R and 39R, which represent the Mogán Group, also suggest that the amount of reworked material constitutes <20 vol% and possibly <10 vol% of the total mass of volcanic clasts supplied to the basin. This is relatively high when compared to the very small amount of volcanic detritus supplied to both the northern and southern basins during the late Miocene nonvolcanic hiatus. This is most likely because of the abundance of explosively generated and (until lithification by welding and devitrification) poorly consolidated pyroclastics generated during the Mogán interval.

Of the total number of volcaniclastic units so far defined between P1 and the Fataga volcaniclastic layers, for example, between ~14 and 11.5 Ma, we tentatively classify 50% as reworked in all three holes. They make up probably <20% by volume, however, because of their generally much smaller thickness. The relative proportion of reworked to primary volcaniclastic layers, however, varies systematically with the stratigraphy in all three sites. As expected, reworked volcaniclastic sediments are in general more abundant in the Fataga interval compared to the Mogán. Local traces of vegetation in epiclastic volcanic sediments in the Fataga Group and more abundant reworking on land also suggest that the climate might have been wetter during Fataga compared to very dry climate prevailing during Mogán time (Schmincke, 1969b, 1994). More importantly, the time between eruptions was generally much larger than during the Mogán stratigraphic interval. In detail, we can identify short periods of volcanic quiescence within the groups, such as between P1 and V in all three cores and, within the Fataga stratigraphic interval.

A diagnostic criterion for erosional downcutting on the island is the appearance and abundance of basaltic lithoclasts in tuffs of the Mogán and Fataga intervals, periods when there was little basaltic

volcanic activity on land. In the southern sites, basaltic lithoclasts, mostly tachylitic to fine-grained basalt, are abundant in most volcaniclastic units below V-type tephra layers. The sources for these lithoclasts were not only "nunatak"-type morphologic islands of Miocene shield basalts that had not been covered by P1 and R ignimbrite sheets but also the upper basaltic portions of P1 and R themselves and the local basalt unit T3.

In contrast, in the two southern Holes 955A and 956B, crystallized to tachylitic basalt is almost absent in volcaniclastic layers between V and A. The widespread but thin basaltic unit T4 was emplaced at 13.6 Ma. just prior to ignimbrite A and locally, such as at Aguimes in eastern Gran Canaria, basalt was also erupted following A. As expected, basaltic lithoclasts are slightly more abundant in tuffs from this interval. Basaltic lithoclasts are almost lacking again in volcaniclastic layers representing the Upper Mogán and Lower Fataga in the southern sites. In contrast, basaltic lithoclasts are common in volcaniclastic layers at Hole 953C, most likely because of the incomplete cover of the highly dissected basaltic shield edifice in eastern and northeastern Gran Canaria by the Mogán and Fataga ignimbrites and the more channelized transport through a postulated caldera outlet in the northeast. Source mixing and reworking can thus be recognized much more easily in the Hole 953C volcaniclastic deposits than in those from the two southern holes, where the subaerial shield basalts remained almost completely buried until deeper canyons were cut during more intense erosional processes during Late Fataga and the volcanic hiatus between Fataga and Roque Nublo volcanic periods.

A process that is difficult to assess concerns major steam explosions generated when thick hot ash flows entered the sea, possibly excavating deep enough into the underlying seabed to repeatedly generate fragments from deposits of the preceding basaltic shield phase.

An estimate of the extent of erosion between successive emplacement of ignimbrites depends on a number of factors, but mainly (1) time between eruptions, (2) climate, and (3) degree of resistance of erosion, chiefly controlled by the thickness of cooling units and their emplacement temperature controlling the degree of welding and crystallization. Any estimate of the extent of erosion thus depends principally on the contrast in glass composition, mineral assemblage, and mineral composition between successive cooling units.

Volcaniclastic Layers Related to Entry of Lava Flows and Debris Avalanches into the Sea

Debris Avalanche Deposits

Deposits have been drilled at all sites that contain angular to rounded fragments of trachyphonolitic lava, up to several centimeters in diameter, set in a nannofossil ooze matrix (e.g., Cores 157-953C-50R, 47R, 46R, and 35R (10.4–12 Ma); Cores 157-956B-31R, 29R, 28R, 26R, 22R, and 21R (9.4–7.3 Ma)). Some of these units exceed 1 m in thickness and most likely were emplaced by mass flows and some by sliding. These deposits could be related to either the entry of subaerial lava flows into the sea or to that of debris flows or lahars generated on land, possibly triggered by flank collapse of the source volcano. Stratigraphically, they occur during the waning stage of Fataga volcanism between ~11 and 9 Ma. Several debris-avalanche deposits transitional to debris-flow deposits have been recognized on land in this time interval (Schmincke, 1994); the coarse submarine deposits may be their distal submarine equivalents.

Lava Flows

We interpret some of the black units in Cores 157-956B-33R through 35R as related to the emplacement of trachyphonolitic lava flows. Firstly, the fragments are entirely of lava, with no ignimbrite fragments present, and the lava fragments are compositionally homogeneous. Secondly, the fragments are angular and thus are not related to redeposited beach pebbles. The biostratigraphic age of the units is compatible with this interpretation, because lava flows of the same age have been dated on land (Bogaard and Schmincke, Chap. 11, this volume).

At least one 17-cm-thick unit (17; Section 157-956B-42R-3) consists of >50 vol% of partly glassy to fully crystallized angular rhyolitic clasts associated with the diagnostic mineral assemblage of Na-rich anorthoclase, ortho- and clinopyroxene, magnetite and zircon. These clasts are most likely derived from the lava flows VL. Because this unit is compositionally homogeneous and because the clasts are angular, we believe the particles were generated almost instantaneously when the lava flow entered the sea. This paucity of volcaniclastic units related to VL lavas is not surprising, because the entrance of this lava flow into the sea was likely restricted to a 5–10 km segment along the southern coast between Barranco de Tasarte and Barranco de Tasartico and at the mouth of Barranco de Tirajana in the southeast. The southern drill Site 955 is away from these likely areas of entry of the lava flow.

Black Units at Hole 956B

Four black sandstones, with thicknesses of 94, 88, 32, and 116 cm, occur in Core 157-956B-32R. They are composed dominantly of primitive basalt, based on their petrography and bulk-rock major and trace element as well as pyroxene chemical composition. They are more primitive than the most mafic sideromelane shards in the Mogán interval in all three sites. The age of these black, basaltic sandstones is ~12 Ma. The predominance of large tachylitic clasts and completely altered sideromelane shards and the paucity of rounded crystallized basalt clasts suggest that these grain-flow deposits were generated either when basaltic lava flows flowed into the sea or when subaerial basalt sections collapsed.

There are two possible sources for these deposits. Basalt lava flows are almost completely absent in the extremely well-exposed subaerial sequence of the Fataga Group throughout southern Gran Canaria, except for a local occurrence of two thin nephelinite lava flows in lower Barranco de Tirajana (Schmincke, 1994). The highly alkaline composition of the basaltic sandstone (Zr/Nb ratio ~4) would be compatible with derivation from these nephelinite flows. However, the otherwise complete absence of mafic lava flows in the Fataga makes it unlikely that such lava flows on Gran Canaria could have been the source for these deposits, although we cannot exclude erosion of such flows from the western and southwestern part of the island. Moreover, the occurrence of plagioclase phenocrysts in some basalt clasts contrasts with the absence of plagioclase in the Fataga nephelinite.

Another possible source is the island of La Gomera, which became covered by basaltic shield lavas between ~10 and 12 Ma (Abdel-Monem et al., 1971; Cantagrel et al., 1984). We speculate that the entry of such lava flows into the sea, the formation of lava deltas, and their subsequent collapse and/or larger scale collapse of part of the island during the shield-building phase may have generated slumps and debris flows whose distal ends were drilled at Site 956. We cannot, however, exclude the possibility that shield basalt activity may have begun at this time in Tenerife and could have been the source for these basaltic sandstones. More precise dating and chemical characterization of the basalts on La Gomera and Tenerife is critical for our tentative interpretation.

Tsunami Deposits

The tentative interpretation of the "exotic" sandstones in the basaltic shield sequence at Hole 956B as tsunami deposits (Schmincke and Segschneider, Chap. 12, this volume) raises the question of whether other tsunami deposits can be recognized and are likely to have been generated during the evolution of the island. Tsunamis are known to transport beach sands on the most proximal shore up to great heights. In the Hawaiian islands (Lanai) such deposits were rec-

ognized as high as 375 meters above sea level (masl; Moore and Moore, 1988). The rebound or backlash wave front can push water many tens of meters inland of the source island. Site 956 is situated 118 km east of La Gomera and 60 km southwest of Gran Canaria. A major ignimbrite entering the sea around the entire southern coast of Gran Canaria is likely to have generated a major tsunami that may travel with a velocity of several 100 km/h. The classic tsunamis resulting from the entry of pyroclastic flows into the sea are those generated by the eruption of Krakatau volcano in August 1883 (Fiske and Simkin, 1983). Those tsunamis, with velocities of 600 km/hr extended as much as 3 km inland, and drowned 36,000 people along the shorelines of Sumatra and Java.

Tsunamis may have formed around Gran Canaria when any one of the larger ignimbrites entered the sea during Mogán and Fataga time. To the east, the tsunamis would have had a major effect on washing beach sands up Fuerteventura, and a returning wave is likely to have reached Gran Canaria in the northeast. The waves propagating from the southwest part of the island would have impacted on the island of La Gomera, where exposed rocks were probably dominantly plutonic rocks, such as syenites, now largely covered unconformably by younger volcanic rocks (Cantagrel et al., 1984). Upon retreat, these sands would have backwashed into the depositional basin between La Gomera and Gran Canaria while the returning wave is likely to have inundated the freshly deposited ignimbrites on land (Fig. 10).

The effect of the temporary water cover would have been manifold. Inundation of the hot ignimbrite would lead to rapid cooling of the mass below the glass transition temperature and cracking and granulation because of thermal shock. Where larger amounts of water would have penetrated jointing cracks or gotten trapped between successive flow units, steam explosions probably generated additional volumes of blocky, glassy shards. Loose, unwelded pumice and shards from the upper part of the ignimbrite would have become washed into the sea, adding to any pumice raft already present. The denser, sand- and lapilli-sized material probably accumulated in large unstable piles that would episodically collapse and be transported in mass flows containing varying amounts of nannofossil mud into the adjacent basin, some scoured from the steep flanks of the seamount. Simultaneously, grinding of pumice rafts would generate a constant shower of glass shards whose sedimentation rate would have far exceeded that of the plankton sedimentation. If this scenario is realistic, we would expect a common association of sand- to lapilli-sized coarse deposits, resulting from the rapid deposition of quenched, vitrified, and fragmented ignimbrites in the shore zone, overlain by varying thicknesses of vitric tuffs composed of bubble-wall shards and varying abundance of pumices. Such sequences are indeed common in all three drill sites (Fig. 10).

Regional Distribution of Mogán and Fataga Pyroclastic Rocks

There are major differences between the volcaniclastic stratigraphy in the north (Site 953) and south (Sites 955 and 956). For example, deposits from the Lower Mogán time interval are almost entirely missing at Site 953. These and other differences are more easily explained when we compare the regional differences in the land record. Nearly all ignimbrites in the Mogán Group are sheets that once covered the entire southern half of Gran Canaria, outside the caldera margin, an area measuring 40 km from east to west and some 20 km from the caldera rim to the present shoreline. In the northeastern quadrant of Gran Canaria, however, most of the rocks of the Mogán Group and a major part of those of the Fataga Group have either been eroded or are covered by younger volcanic rocks. Only at San Lorenzo and Miraflor are very small remnants of Mogán rocks exposed, with the San Lorenzo section showing an extremely condensed Mogán sequence of <15 m total thickness. Volcanic deposits representing the upper part of the Lower Mogán Formation are missing. On the other hand, we think that ignimbrites in the northeast were primarily transported through canyons, because the shield basalt terrain was highly dissected in this area. The channelling of the ignimbrites had several consequences: (1) nondeposition on the higher slopes and generation of condensed sections, (2) greater degree of erosion in the subaerial barrancos continuing into submarine canyons, and (3) higher mass entry rates where the pyroclastic flows debouched into the sea. Whether or not submarine transport from the Miocene shoreline was via submarine canyons to the foot of the steep submarine slopes prior to spreading in the flat basin, as it is today, or whether they spread in the form of turbidite sheets down the flanks is not known.

Concentric vs. Channelized Sedimentation

It is surprising that the great thicknesses of Mogán and Fataga volcaniclastic units were drilled at Site 953, 70 km northeast of the present shoreline. The extremely limited outcrops of these rocks in the northeastern section of the island appear to suggest that the bulk of the ash flows erupted south and southwest of the Miocene caldera. We speculate, however, that limited deposition on land may not reflect mass effusion rates of the ash flows in the northeastern sector. The old shield basalts in the northeastern sector of the island had been strongly eroded prior to eruption of the ash flows, contrasting with the almost completely undissected nature of the younger Tasartico shield in the southwest. Here, the thickness of individual ignimbrite sheets varies very little, except for the Horgazales Basin in the southwest where ignimbrites were ponded, and hence similar mass entry rates into the sea are assumed for the southern sector.

The mass of ash flows that enters the sea per unit length and unit time can generally not be quantified very well, except for using the inferred velocity of an ash flow and, where available, the cross section of a canyon through which ash flows debouch into the sea. Rough preliminary calculations suggest that a volume in excess of that deposited on land entered the sea.

Sideromelane and Hyaloclastites

The occurrence of sideromelane and hyaloclastites within felsic ash layers was unexpected. Sideromelane shards occur almost exclusively in submarine tephra layers corresponding to the Mogán stratigraphic interval in all holes, but most commonly in Site 955. Very few were found in Fataga phase volcaniclastic layers. Perhaps disturbances of the volcano/magma system associated with the greater magnitude of ash flow eruptions during the Mogán phase triggered the submarine basaltic eruptions.

The occurrence, composition, and interpretation of sideromelane shards are discussed in this chapter because they are intimately mixed with felsic volcaniclastics in all layers and their occurrence is pertinent for understanding the emplacement mechanism of volcaniclastic units. We have analyzed fresh sideromelane shards by microprobe in 26 polished sections from all sites and selected only analyses with totals higher than 98.5 wt% in our plots (Figs. 11–15; Table 1). For analytical conditions see Sumita and Schmincke (Chap. 15, this volume). Volcaniclastic units from Holes 955A and 953C are well represented, but only three samples containing sideromelane shards were analyzed from Hole 956B. For comparison, we have re-analyzed and plotted whole-rock compositions of four basalts from the Mogán Group (Fig. 11). The bulk of the sideromelane compositions range between 4 and 6 wt% MgO, but more magnesian compositions occur at all holes, up to 8 wt% in Hole 956B.

The compositions fall into two main groups on the mafic end. Alkali basalts dominate at all holes. A second, tholeiitic group, is clearly distinguished in all major oxides from the alkali basalt and is most common at Hole 953C; tholeiitic to transitional sideromelane populations also occur in Hole 955A and Hole 956B. The main chemical characteristics of the tholeiitic glasses are K_2O as low as 0.4 wt%, lower CaO, FeO*, TiO_2, and P_2O_5 concentrations, and higher SiO_2. At

the other end of the spectrum, a group of sideromelane shards very rich in alkalis (VU-36, Hole 955A) is distinguished from the other groups by high K_2O, Na_2O, Al_2O_3, P_2O_5, and CaO concentrations.

The volatile elements F, Cl, and S were measured in all polished sections in which sideromelane was analyzed. There are three major factors that need to be considered when interpreting the volatile concentrations: degree of alkalinity of the magma, degree of differentiation, and degree of degassing. We have not yet compared the volatile concentrations with the vesicularity of the shards for an independent check of the degassing, so our conclusions are tentative.

The difficulty in arriving at a straightforward interpretation is well illustrated by comparing subalkaline (K_2O < 1 wt%) and relatively mafic (MgO > 5.5 wt%) sideromelane compositions in two different sites. Sideromelane from VU-14 (Lower Mogán, Hole 953C) is one of the most depleted (K_2O ~0.5 wt%) and at the same time most mafic (MgO 5.7–6.4 wt%) samples, while sideromelane from VU-15 (Hole 955A) is slightly less mafic (MgO < 5.8 wt%) and slightly more potassic (K_2O > 0.8 wt%). The third sample is from VU-45 (Hole 956B) (MgO 5.7–8 wt%, K_2O 2–0.5 wt%).

The most subalkaline sideromelane from Hole 953C is also the one with the lowest sulfur, fluorine, and chlorine concentrations, and shards from VU-60 (Hole 953C) show a similar pattern. For the two samples from Holes 956B and 955A, the positive correlation between chlorine and sulfur might suggest degassing of both elements, although the decrease of sulfur is much faster because sulfur is less soluble in the magma than chlorine. The opposite trend found in the two subalkaline sideromelane populations at Hole 953C might best be explained by the fact that sulfur concentration decreases with increasing differentiation while chlorine concentrations increase. Fluorine, the least soluble of the three volatiles discussed here, shows a more regular relationship. For most sideromelane populations from the different volcaniclastic layers, fluorine correlates negatively with MgO and positively with K_2O. We have speculated elsewhere (Gurenko and Schmincke, Chap. 25, this volume) on possible contamination by seawater of magmas from which Pleistocene sideromelane at Sites 953, 954, and 956 were derived. A more detailed assessment of the volatile concentration in the Miocene sideromelane glasses will be delayed until we have more fully assessed the relationship between vesicularity and volatile concentration and the heterogeneity in sideromelane compositions in several samples.

The occurrence of these fresh sideromelane shards, which erupted concurrently with the Mogán and Lower Fataga ignimbrites on land, strongly suggests that submarine basaltic volcanic activity occurred all around the submarine cone of Gran Canaria. In other words, during the stage of post-shield volcanism the island grew by both subaerial and submarine surface volcanism apart from plutonic growth in its interior. The total volume of sideromelane shards mixed with felsic volcaniclastic shards at all three sites is not large and would probably amount to not more than a few meters of densely packed sideromelane shards at the drill sites if it were all concentrated in one layer. The depositional site on the flat bottom of the depositional basins is, however, tens of kilometers away from the likely site of eruption along the middle and lower slopes of the island. We thus have to reckon with the fact that the submarine slopes during this volcanic phase were dotted with basaltic cones and/or lava flows.

At the present scale of interpretation, we did recognize major differences between the compositions of the Miocene sideromelane shards (this paper) and those analyzed from Pleistocene ash layers (Gurenko and Schmincke, Chap. 25, this volume). Interestingly, however, the only hyaloclastite ash layer dominated by sideromelane shards among the young ash layers occurs in Hole 953A (Sample 157-953A-16H-2, 45–47 cm) and is much more depleted than the other sideromelane compositions, although still more alkalic than the tholeiitic shards which are also most common at Hole 953C.

Significantly, sideromelane shards in both the Miocene and Pleistocene volcaniclastic layers are never very mafic, most MgO concentrations being between 4.5 and 6.5 wt%. Provided that most sideromelane shards represent true submarine eruptions, for which evidence for the Miocene ash layers is excellent but for the Pleistocene sideromelane shards equivocal, we note that basaltic submarine flank eruptions on Gran Canaria, and for the Pleistocene sideromelane shards at Site 956 and also Tenerife, are selective in the sense that no primitive magmas are erupted.

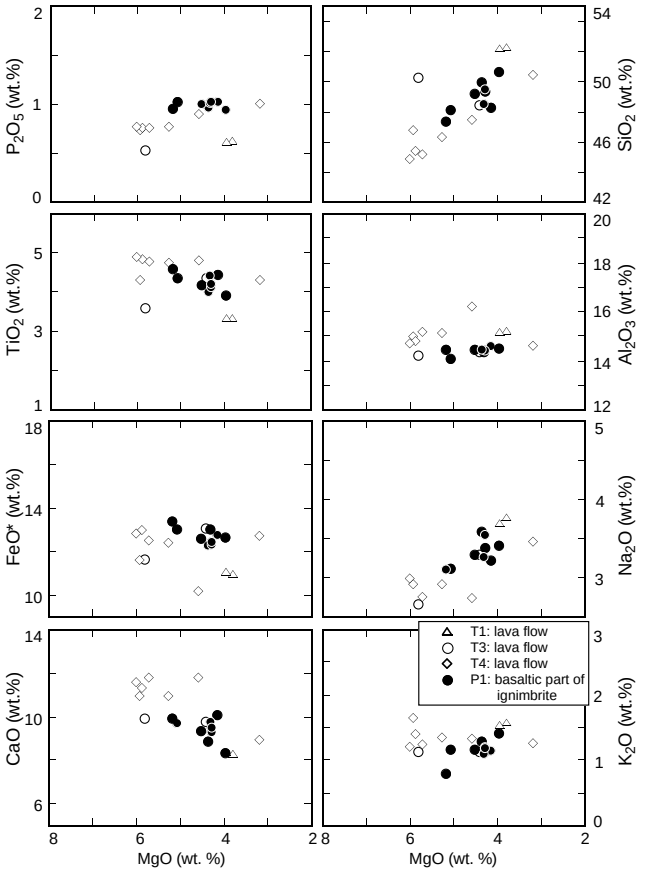

Figure 11. MgO vs. major elements of basalts from the Mogán Group (Gran Canaria).

Submarine Eruptions

We suggest that most sideromelane ash particles found within felsic volcaniclastic layers at all three sites were formed by submarine eruptions, because there is an almost complete absence of basalt flows on land, except for the widespread rhyolite-basalt composite ignimbrites, P1 and R, and spatially restricted T3 and T6 basalts. We know of only one widespread basaltic event (T4) that occurred between the eruptions of ignimbrites O and A at the base of the upper Mogán Formation.

We cannot deny that basaltic hyaloclastite cones formed at the shore and were subsequently eroded. We consider this hypothesis unlikely, however, because the only basaltic dikes known to have traversed part of the cooling units of the Mogán Group are those associated with the widespread basaltic eruptive event of T4. We therefore conclude that the sideromelane shards in the felsic volcaniclastic layers of Holes 953C, 955A, and 956B are the result of submarine eruptions.

It is also possible that the basaltic glass shards in the felsic volcaniclastic layers are derived from the thick hyaloclastite carapace that

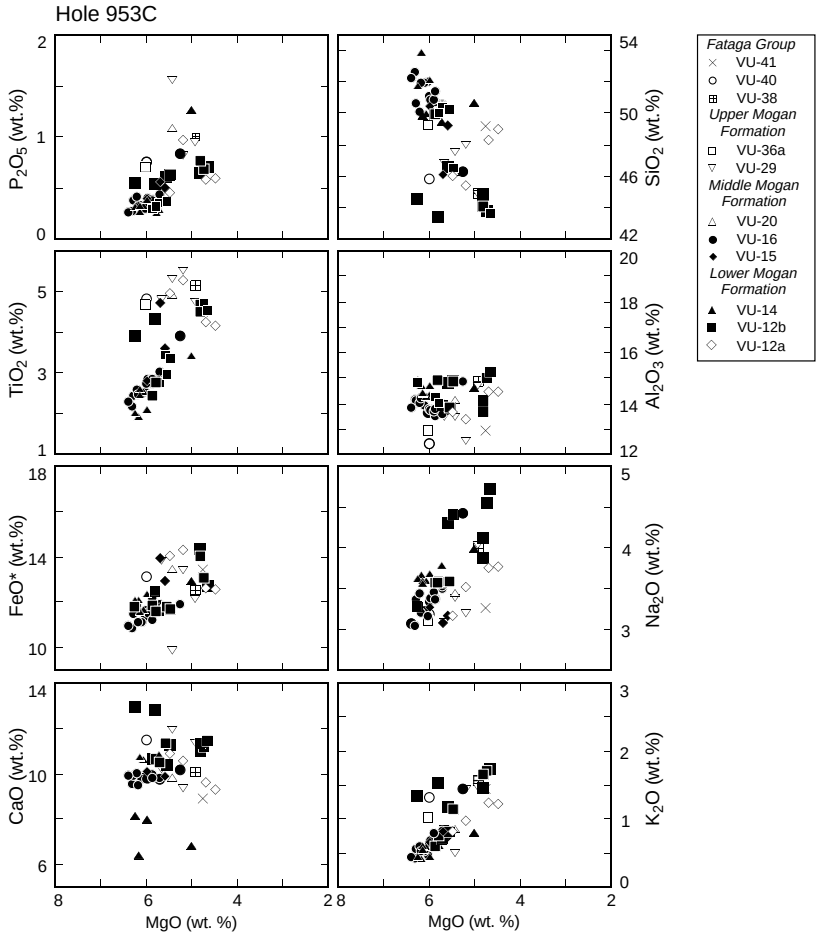

Figure 12. MgO vs. major elements of sideromelane shards from Hole 953C. Samples include VU-41 (Sample 157-953C-61R-3, 109–114 cm), VU-40 (Sample 157-953C-62R-1, 100–118 cm), VU-38 (Sample 157-953C-63R-1, 40–48 cm), VU-36 (Sample 157-953C-64R-3, 72–75 cm), VU-29 (Sample 157-953C-66R-3, 16–22 cm), VU-20 (Sample 157-953C-67R-4, 53–59 cm), VU-16 (Sample 157-953C-68R-3, 60–66 cm), VU-15 (Sample 157-953C-68R-4, 56–60 cm), VU-14 (Sample 157-953C-69R-1, 0–7 cm), VU-12b (Sample 157-953C-69R-2, 75–81 cm), and VU-12a (Sample 157-953C-69R-4, 22–29 cm).

mantled the Gran Canaria seamount prior to inception of felsic volcanism. Such scouring of the hyaloclastite substrate occurred, as shown by fragments of altered, glassy shards or pieces of indurated hyaloclastite tuff. We exclude this possibility, however, because the sideromelane shards in the felsic volcaniclastic units are extremely fresh, clear, yellow glass, whereas former sideromelane shards or fragments of hyaloclastite tuff are completely altered and chemically and mineralogically homogeneous. We have not found fragments that show the transition from sideromelane to tachylite in individual clasts as would be expected in particles derived from the disintegration of, for example, pillow lavas.

At What Depth Did the Submarine Basaltic Eruptions Occur?

The exact depth of the submarine basaltic eruptions is difficult to specify but may have been as deep as 1000 m, because these basaltic magmas are not only alkalic, where explosive eruptions are estimated to occur as deep as ~700 meters below sea level (mbsl; Staudigel and Schmincke, 1984) or 500 mbsl (Binard et al., 1993), but they are also moderately evolved so their volatile concentrations had probably been enriched as well.

The evidence for many submarine eruptions of moderately evolved basalts throughout Mogán time suggests that these Fe-rich, dense magmas may be the parental magmas for mafic trachyte magmas, commonly the least evolved magmas erupted as ignimbrites. This neither implies nor excludes the possibility that the mixed sideromelane and rhyolitic or trachytic shards reflect synchronous submarine and subaerial eruptions. The abundance of sideromelane shards in several units and their general freshness do indicate, however, that the basalt eruptions could not have occurred long before the eruption of a particular ash flow on land.

Where, When, and Why Did the Mixing Between Felsic and Basaltic Shards Occur?

No sideromelane shards have been found associated with the widespread emplacement of P1 and R ignimbrites, both of which consist of >50% basalt (Freundt and Schmincke, Chap. 14, this volume). Hence, submarine basaltic eruptions at this stage are not documented and may not have occurred, perhaps because it was easier at this time for basaltic magmas to erupt through the center of the island before a large low-density magma volume in the reservoir had developed.

The composition of sideromelane shards varies greatly between felsic volcaniclastic layers. Where sideromelane shards have the same composition in one sample, the eruption likely occurred almost synchronously with the passage of the ignimbrite-generated ash turbidite. Heterogeneous compositional populations, on the other hand, might indicate either multiple mixing events, eruption of a zoned magma, or multiple sources. Most likely, the most heterogeneous samples represent eruption of magmas from different sites and erosion of several eruptive sites (submarine cones?) by the turbdite passing by and mixing during transport.

We interpret the nearly complete absence of sideromelane shards from Fataga volcaniclastic units as evidence for a more deep-seated basaltic magma reservoir and/or thick low-density plug in the core of the island, which had grown downward by more abundant formation of felsic plutonic rocks in view of the larger noneruptive intervals.

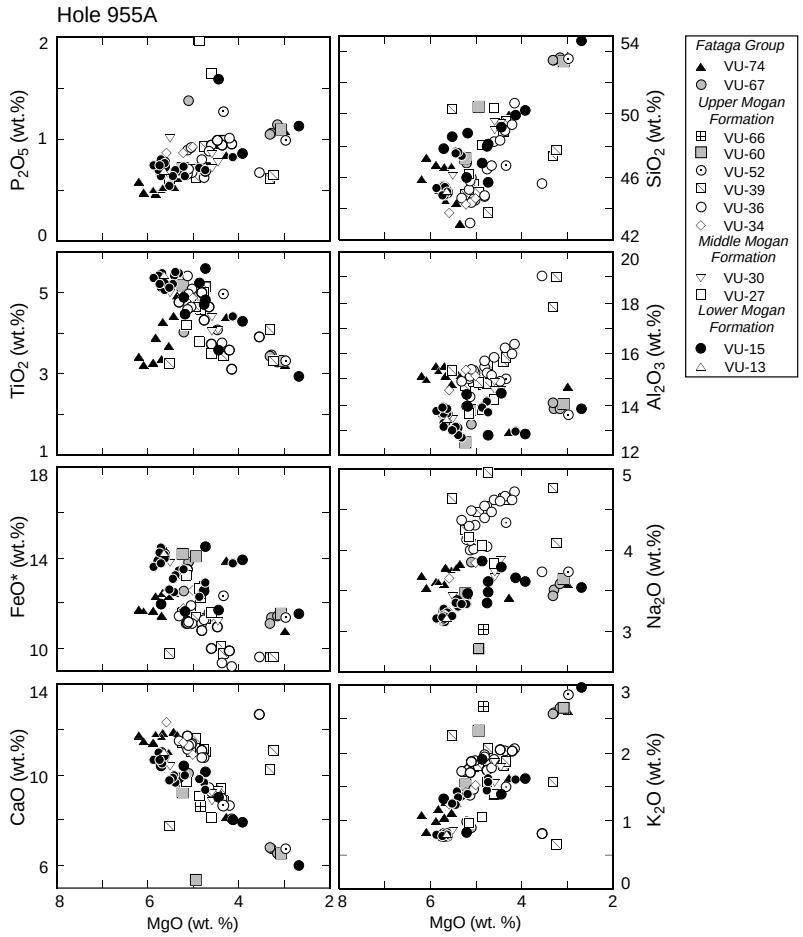

Figure 13. MgO vs. major elements of sideromelane shards from Hole 955A. Samples include VU-74 (Sample 157-955A-54X-CC, 10–14 cm), VU-67 (Sample 157-955A-55X-4, 19–25 cm), VU-66 (Sample 157-955A-55X-4, 19–25 cm), VU-60 (Sample 157-955A-56X-3, 16–25 cm), VU-52 (Sample 157-955A-57X-2, 104–110 cm), VU-39 (Sample 157-955A-58X-1, 16–17 cm), VU-36 (Sample 955A-58X-1, 86–90 cm), VU-34 (Sample 157-955A-58X-1, 119–125 cm), VU-30 (Sample 157-955A-58X-4, 71–76 cm), VU-27 (Sample 157-1955A-58X-5, 72–78 cm), VU-15 (Sample 157-955A-59X-6, 61–67 cm), and VU-13 (Sample 157-955A-59X-6, 128–140 cm).

The more alkalic parent magmas for the Fataga volcanics reflect a major change in source from Mogán to Fataga time, possibly to greater depths.

CONCLUSIONS

The most striking clasts found in the volcaniclastic sediments drilled from the volcanic apron of Gran Canaria are dense, blocky, angular brown shards that occur in tuff and lapillistone turbidites that can be correlated to widespread ignimbrite sheets on land. Many of those volcaniclastic deposits containing such shards also contain more roundish ash-sized to rarely lapilli-sized clasts clearly composed of shards that are welded together to varying degrees. The dense, blocky shards are interpreted to have been derived from strongly welded ash flows either when the flows entered the sea or from their interiors as they were rapidly eroded along the shoreline, repeatedly exposing the strongly welded but not yet devitrified glassy interior. Very high emplacement temperatures of the Gran Canaria ignimbrites is implied by their densely welded basal vitrophyres and strongly crystallized interiors (Schmincke and Swanson, 1967; Schmincke, 1974). Each ash flow must have entered the sea, however, as a relatively dense mass of glass shards, megafiamme in some ignimbrites (C, D, and E) exceptionally exceeding 5 m (!) in length, and slightly inflated lava lumps. Arguments for an inflated transport of P1 ignimbrite are discussed elsewhere (Freundt and Schmincke, 1995). We do not know how far the dense, hot ash flows continued into the water prior to becoming fragmented. Judging from the large volume and the high velocities of the flows, we estimate that the momentum carried the flows at least several hundred meters, possibly >1 km into the sea before freezing shut. Fast cooling would inevitably lead to overall rapid freezing at the frontal areas and buildup of an inherently unstable barrier that might have formed some sort of temporary “reef” fringing the island. In such a mass that grew upward and forward as successive flow units were emplaced on top of each other, domains of strong welding and lesser welding were likely to have been juxtaposed in a chaotic manner. Trapping of water between flow units, below collapsed portions of the “reef” and water that penetrated into cooling cracks, would have led to widespread steam explosions that tended to fragment the piled-up ash flow masses which ranged from hot to quenched with extremely chaotic temperature distributions and locally very steep thermal gradients. Layer by layer of the mounds and large blocks that may have been formed by steam explosions would have cracked by thermal shock and spalled off as the hot interior became repeatedly exposed to seawater. Following emplacement, erosional cliffs must have formed along the periphery of the island, where the hot interior of ignimbrites became exposed time and again, quenched, and fragmented until they had cooled to ambient temperature. Cooling times for the subaerial ignimbrite sheets, assuming an emplacement temperature of 700°–800° C and an average thickness of 20 m, are on the order of 50 yr (Kobberger and Schmincke, in press).

The incipiently welded clasts found in the tuffs are thought to be derived from the upper part of the cooling unit, and the strongly welded ones more likely from the postulated large chaotic mounds. We speculate that the spectacular ramp structures in the upper part of many subaerial ignimbrites (Schmincke and Swanson, 1967) may have formed in response to the rapid freezing at the front of the thick ash flows leading to deceleration of a flow and increasing sliding of thick layers.

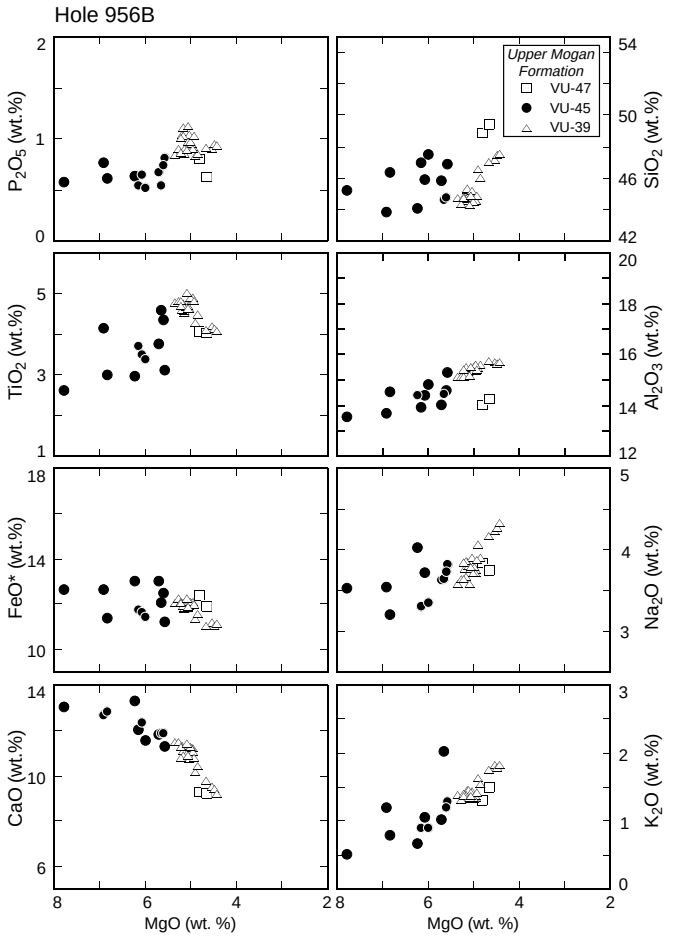

Figure 14. MgO vs. major elements of sideromelane shards from Hole 956B. The MgO variation diagram shows major and trace elements of sideromelane shards from Hole 956B. Samples include VU-47 (Sample 157-956B-39R-2, 114–118 cm), VU-45 (Sample 157-956B-39R-2, 114–118 cm), and VU-39 (Sample 157-956B-40R-1, 68–71 cm).

We thus expect that the highest volume of mass transfer of glassy particles to the deep sea is directly related to the entry of the ash flows into the sea with a still high but diminishing rate lasting for ~50 yr. The relative proportions of dense, blocky shards and more normal bubble-wall and tricuspate shards would thus mainly depend on the emplacement temperature and thickness of an ash flow sheet. It is not clear whether the common fine-grained vitric tuffs consisting of >90 vol% bubble-wall shards are due mainly to sorting during turbidite transport, to fallout from highly explosive eruptions, to shearing at the base of ash flows traveling over the water, or to co-ignimbrite ash clouds.

The emplacement of ash flow sheets is believed to have differed significantly between the southern circumference of Gran Canaria, where the sheets covered almost undissected terrain between ~14 and 13.3 Ma, and the northeast part of Gran Canaria, where ash flows are thought to have been delivered to the sea through one or more major canyons of the previously dissected, basaltic shield volcano. Because of this contrast, several ignimbrites that appear as ponded flows within the caldera basin in the south are presented by volcaniclastic units at Hole 953C, but are absent as tuff layers from Holes 955A and 956B. Nevertheless, the occurrence of most ignimbrites at all three drill sites suggests that concentric sedimentation around the island occurred 20 to 30 times during one, and possibly several million years.

Submarine, syn-ignimbrite tephra layers that are reasonably fresh, such as those drilled, have preserved a number of characteristics that have mostly or completely disappeared in the ash flow deposits that cooled and devitrified on land. Most important is the abundance of glass preserved by quenching as the shard and pumice populations entered the sea. The transient vitric stage lasted only a few years in the subaerially deposited ash flows, except for a basal vitrophyre generally <20 cm thick and commonly completely smectitized during diagenesis. Following drilling of Leg 157, we made a special effort to search for minute quantities of fresh glass in many argillized vitrophyres at the base of many ignimbrites on Gran Canaria and have reported the results of microprobe analyses of fresh glass in the companion paper (Sumita and Schmincke, Chap. 15, this volume). The glassy, primary, unwelded shards and pumice lapilli in the submarine tuffs, however, allow characterization of the shape and vesicularity of primary particles as they appeared during subaerial transport. Reconstruction of these primary features is a major problem in all ignimbrites emplaced hot that become strongly welded and devitrified in

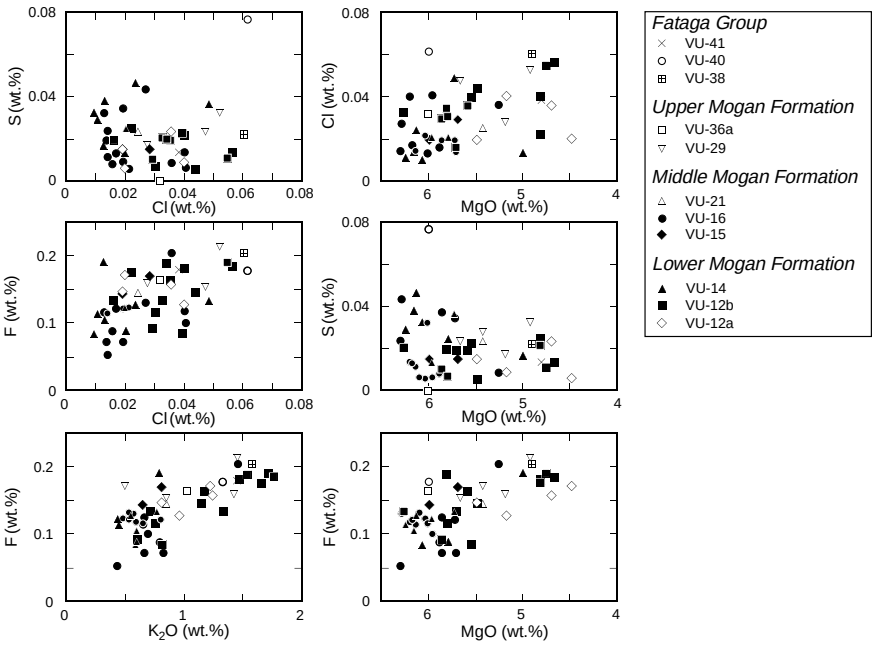

Figure 15. S, F, and Cl concentrations vs. MgO and K_2O for sideromelane shards from Hole 953C. For sample numbers see Figure 12.

Table 1. Representative EMP analyses of sideromelane shards from Holes, 953C, 955A, and 956B.

Hole, core, section:	953C-69R-4	953C-69R-4	953C-69R-2	953C-69R-2	953C-69R-2	953C-69R-2	953C-69R-1	953C-69R-1	953C-68R-4	953C-68R-3
Interval (cm):	22-29	22-29	75-81	75-81	75-81	75-81	0-7	0-7	56-60	60-66
Depth (cm):	835.58	835.58	833.74	833.74	833.74	833.74	831.10	831.10	826.07	824.66
Volcaniclastic unit:	VU-12a	VU-12a	VU-12b	VU-12b	VU-12b	VU-12b	VU-14	VU-14	VU-15	VU-16
Sample number:	SD-1	SD-4	SD-2	SD-3	SD-7	SD-12	SD-1	SD-3	SD-1	SD-2
Number of analyses:	3	3	3	3	3	4	3	3	6	2
(wt%)										
SiO_2	45.11	49.07	44.74	46.65	50.11	43.05	50.40	49.21	49.10	51.93
TiO_2	5.25	4.17	3.95	3.44	2.78	4.48	2.55	2.84	3.58	2.16
Al_2O_3	13.28	14.49	14.93	14.83	14.04	15.08	14.40	13.96	13.67	13.99
FeO*	14.22	12.58	11.88	11.69	11.61	12.57	11.76	11.76	12.91	10.72
MnO	0.22	0.21	0.22	0.17	0.17	0.16	0.17	0.15	0.22	0.20
MgO	5.14	4.49	6.30	5.60	5.80	4.60	6.11	5.69	5.59	6.22
CaO	10.49	9.32	13.01	11.36	10.66	11.31	10.73	10.81	9.85	9.43
Na_2O	3.50	3.78	3.30	4.31	3.60	4.66	3.62	3.76	3.15	3.01
K_2O	0.96	1.23	1.35	1.18	0.75	1.73	0.59	0.77	0.73	0.43
P_2O_5	0.96	0.59	0.56	0.61	0.32	0.70	0.32	0.28	0.50	0.27
BaO	0.068	0.110	0.092	0.097	0.084	0.129	0.123	0.126	0.058	0.047
S	0.008	0.006	0.021	0.020	0.007	0.013	0.033	0.036	0.078	0.024
Cl	0.040	0.020	0.033	0.035	0.030	0.056	0.010	0.048	0.039	0.014
F	0.127	0.171	0.135	0.164	0.117	0.184	0.084	0.131	0.124	0.052
Total:	99.37	100.22	100.52	100.16	100.08	98.72	100.92	99.57	99.80	98.67

Table 1 (continued).

Hole, core, section:	953C-68R-3	953C-67R-4	953C-66R-3	953C-66R-3	953C-65R-6	953C-64R-3	953C-63R-1	953C-62R-1	953C-61R-3	955A-59X-6
Interval (cm):	60-66	53-59	16-22	16-22	103-107	72-75	40-48	100-118	109-114	128-140
Depth (cm):	824.66	816.49	805.03	805.03	800.02	786.14	773.5	764.6	758.06	559.98
Volcaniclastic unit:	VU-16	VU-21	VU-29	VU-29	VU-31	VU-36	VU-38	VU-39	VU-41	VU-13
Sample number:	SD-4	SD-2	SD-2	SD-5	SD-1	SD-2	SD-2	SD-6	SD-1	SD-1
Number of analyses:	2	2	2	2	2	2	3	3	3	2
(wt%)										
SiO_2	49.66	45.82	46.48	43.69	47.81	48.93	44.58	45.03	48.99	44.71
TiO_2	2.89	4.87	4.75	4.61	3.15	4.64	5.10	4.73	4.49	5.38
Al_2O_3	13.49	14.00	13.36	14.31	6.30	12.86	14.78	12.20	12.90	13.34
FeO*	11.64	13.34	13.72	11.79	10.43	11.60	12.47	12.88	13.37	14.07
MnO	0.18	0.23	0.20	0.20	0.92	0.17	0.22	0.25	0.23	0.26
MgO	5.61	5.37	5.62	4.79	15.97	5.98	4.87	5.90	4.75	5.59
CaO	9.60	9.74	10.09	11.03	9.51	9.74	9.98	11.30	8.88	10.90
Na_2O	3.43	3.41	3.06	3.92	4.75	3.08	3.97	3.13	3.26	3.14
K_2O	0.81	0.85	0.85	1.42	0.66	1.01	1.56	1.31	1.44	0.78
P_2O_5	0.43	1.07	0.55	0.92	0.09	0.71	0.99	0.74	0.69	0.68
BaO	0.069	0.048	0.040	0.085	0.071	0.118	0.132	0.137	0.091	0.090
S	0.019	0.023	0.023	0.031	0.019	0.000	0.022	0.075	0.013	0.074
Cl	0.014	0.025	0.047	0.051	0.013	0.032	0.060	0.060	0.038	0.036
F	0.071	0.143	0.152	0.207	1.259	0.162	0.202	0.175	0.180	0.133
Total:	98.17	99.15	99.19	97.33	100.94	99.27	99.17	98.14	99.54	99.18

Table 1 (continued).

Hole, core, section:	955A-59X-6	955A-59X-6	955A-59X-6	955A-59X-6	955A-58X-5	955A-58X-4	955A-58X-4	955A-58X-4	955A-58X-1	955A-58X-1
Interval (cm):	61-67	61-67	61-67	61-67	72-78	71-76	71-76	71-76	119-125	86-90
Depth (cm):	559.31	559.31	559.31	559.31	548.32	546.81	546.81	546.81	542.79	542.46
Volcaniclastic unit:	VU-15	VU-15	VU-15	VU-15	VU-27	VU-30	VU-30	VU-30	VU-34	VU-36
Sample number:	SD-2	SD-13	SD-22	SD-25	SD-2	SD-4	SD-6	SD-2	SD-1	SD-3
Number of analyses:	2	2	2	2	2	1	1	2	1	1
(wt%)										
SiO_2	54.35	48.49	45.11	47.52	48.04	49.08	52.16	45.76	44.29	45.61
TiO_2	2.93	4.46	5.14	5.22	3.80	4.02	3.08	4.94	4.92	3.91
Al_2O_3	13.75	13.82	13.78	13.11	13.76	14.44	13.13	13.34	15.38	19.06
FeO*	11.46	11.59	13.87	13.08	12.63	11.12	11.52	13.69	11.754	9.62
MnO	0.22	0.16	0.23	0.19	0.27	0.18	0.23	0.19	0.231	0.10
MgO	2.67	5.16	5.66	5.46	4.87	4.41	2.76	5.45	5.23	3.57
CaO	5.97	9.94	10.47	9.88	9.05	9.20	6.13	10.30	11.42	12.71
Na_2O	3.53	3.45	3.17	3.35	4.05	3.84	2.86	3.40	4.13	3.74
K_2O	2.95	1.39	0.80	1.23	1.06	1.77	2.63	0.84	1.42	0.82
P_2O_5	1.12	0.63	0.76	0.63	1.96	0.76	1.00	0.99	0.86	0.67
BaO	0.096	0.041	0.040	0.104	0.073	0.112	0.137	0.044	0.179	0.060
S	0.038	0.014	0.120	0.001	0.034	0.038	0.051	0.057	0.032	0.011
Cl	0.044	0.040	0.061	0.046	0.046	0.083	0.070	0.052	0.044	0.058
F	0.217	0.147	0.133	0.168	0.232	0.193	0.251	0.192	0.236	0.144
Total:	99.34	99.32	99.35	99.98	99.88	99.24	96.00	99.24	100.13	100.07

Table 1 (continued).

Hole, core, section:	955A-58X-1	955A-58X-1	955A-58X-1	955A-58X-1	955A-58X-1	955A-57X-2	955A-56X-3	955A-56X-3	955A-56X-1	955A-55X-4	955A-55X-4
Interval (cm):	86-90	86-90	16-17	16-17	16-17	104-110	16-25	16-25	14-17	19-25	8-13
Depth (cm):	542.46	542.46	541.76	541.76	541.76	534.54	525.59	525.59	522.54	517.59	517.48
Volcaniclastic unit:	VU-36	VU-36	VU-39	VU-39	VU-39	VU-52	VU-60	VU-60	VU-66	VU-67	VU-67
Sample number:	SD-13	SD-15	SD-18	SD-23	SD-12	SD-13	SD-12	SD-11	SD-1	SD-7	SD-6
Number of analyses:	1	2	1	1	2	1	2	3	2	2	2
(wt%)											
SiO_2	48.34	44.60	46.92	46.98	49.38	45.49	47.27	53.46	46.72	53.61	45.97
TiO_2	3.74	4.75	4.04	3.28	3.20	4.83	5.19	3.33	4.48	3.31	3.96
Al_2O_3	15.86	14.89	17.68	18.70	15.06	14.63	12.54	14.05	14.39	13.83	13.67
FeO*	9.995	11.42	9.533	9.486	9.60	12.025	14.23	11.55	11.88	11.45	12.33
MnO	0.251	0.22	0.229	0.171	0.20	0.195	0.30	0.22	0.20	0.19	0.27
MgO	4.62	5.30	3.28	3.19	5.43	4.23	5.23	3.09	4.72	3.16	5.10
CaO	9.25	11.51	10.15	10.90	7.59	8.45	9.25	6.53	8.39	6.55	9.29
Na_2O	4.62	4.36	4.73	4.02	4.55	4.23	3.48	3.66	2.95	3.58	4.06
K_2O	1.91	1.73	1.56	0.64	2.22	1.46	1.55	2.68	2.61	2.66	0.97
P_2O_5	0.94	0.65	0.61	0.63	0.60	1.23	0.72	1.09	0.70	1.14	1.99
BaO	0.178	0.061	0.128	0.092	0.093	0.106	0.047	0.125	0.060	0.124	0.078
S	0.024	0.003	0.016	0.050	0.013	0.036	0.004	0.005	0.005	0.020	0.048
Cl	0.082	0.073	0.061	0.030	0.055	0.057	0.065	0.047	0.014	0.054	0.046
F	0.254	0.218	0.184	0.124	0.141	0.370	0.222	0.238	0.166	0.231	0.236
Total:	100.05	99.79	99.13	98.30	98.14	97.34	100.09	100.07	97.27	99.91	98.02

Table 1 (continued).

Hole, core, section:	955A-54X-CC	955A-54X-CC	955A-54X-CC	955A-54X-CC	956B-40R-1	956B-40R-1	956B-69R-3	956B-69R-3	956B-69R-3	956B-69R-3	956B-39R-2
Interval (cm):	10-14	10-15	10-16	10-17	68-71	68-71	88-92	88-92	88-92	88-921	14-118
Depth (cm):	503.50	503.50	503.50	503.50	532.98	532.98	525.96	525.96	525.96	525.96	525.00
Volcaniclastic unit:	VU-74	VU-74	VU-74	VU-74	VU-39	VU-39	VU-45	VU-45	VU-45	VU-45	VU-47
Sample number:	SD-15	SD-18	SD-11	SD-13	SD-24	SD-25	SD-2	SD-9	SD-3	SD-8	SD-5
Number of analyses:	2	2	3	3	2	2	2	2	3	3	1
(wt%)											
SiO_2	50.18	45.94	53.30	46.93	47.20	44.18	44.03	45.24	44.32	43.68	48.48
TiO_2	4.41	3.41	3.19	3.27	4.04	4.64	2.98	2.61	4.56	4.13	4.02
Al_2O_3	12.96	15.15	14.60	15.54	15.55	15.19	14.40	13.55	14.36	13.63	13.90
FeO*	13.93	11.75	10.69	11.68	11.03	11.89	13.00	12.68	12.03	12.61	12.28
MnO	0.33	0.19	0.21	0.16	0.16	0.17	0.21	0.16	0.19	0.22	0.21
MgO	4.28	6.20	2.96	5.88	4.40	5.15	6.23	7.80	5.62	6.91	4.77
CaO	8.15	11.74	6.70	11.47	9.10	10.64	13.32	13.07	11.81	12.64	9.23
Na_2O	3.43	3.68	3.54	3.62	4.30	3.80	4.03	3.53	3.63	3.53	3.81
K_2O	1.64	1.08	2.59	0.99	1.82	1.35	0.68	0.51	2.01	1.20	1.29
P_2O_5	0.84	0.58	1.07	0.49	0.93	0.99	0.64	0.58	0.54	0.77	0.79
BaO	0.000	0.099	0.094	0.050	0.127	0.107	0.116	0.017	0.098	0.102	0.117
S	0.025	0.053	0.028	0.053	0.060	0.105	0.011	0.047	0.031	0.002	0.026
Cl	0.028	0.066	0.057	0.039	0.048	0.032	0.034	0.062	0.037	0.024	0.053
F	0.193	0.194	0.188	0.140	0.214	0.177	0.190	0.112	0.156	0.142	0.198
Total:	100.46	100.21	99.26	100.37	99.25	98.69	99.86	99.97	99.39	99.58	99.17

the lower and central part of a cooling unit and intensely modified by pervasive vapor phase crystallization in the less strongly welded top layers. We have begun an image analysis project to study the primary particles with this aim. Secondly, the drastic quenching and fragmentation mechanisms in the proposed near-shore pile-up zone, in the sea cliffs formed soon after eruption and by the postulated backwash waves that temporarily covered the ash flow sheets inland for a brief moment, by thermal shock granulation, and explosions of superheated steam, all preserved a glassy state that did not survive on land in the bulk of the ignimbrites. Finally, phenocrysts unstable during cooling and high-temperature devitrification, such as hypersthene, that are subjected to high-temperature oxidation, such as magnetite, and quenching of phenocrysts containing melt inclusions, tend to be much better preserved in the submarine syn-ignimbrite tephra units.

We have provided abundant evidence that both sideromelane clasts present in many of the volcaniclastic units and one, almost pure, hyaloclastite tuff formed during submarine eruptions at several hundred to several thousand meters below sea level. They provide strong evidence that mafic, parental magmas from which the rhyolitic, trachytic and trachyphonolitic magmas were differentiated were present at the time of ash flow eruption and of the right composition to qualify as parent magmas. These mafic magmas apparently were unable to penetrate the low-density magma reservoir and to erupt on the surface but found outlets along the submarine circumference of Gran Canaria seamount. With a postulated eruption depth of the basaltic magmas of >500 and <4000 mbsl, most of the felsic magmas may have developed and resided in near surface magma reservoirs not >5 km below the surface of the caldera rim unless the dikes feeding the submarine basaltic eruptions completely bypassed the central magma reservoirs.

ACKNOWLEDGMENTS

Walter Hales and Alex Webbers made our many trips to the core repository in Bremen most enjoyable. At GEOMAR, our analytical studies and the final preparation of the manuscripts owe much to the tremendous efforts of Petra Gloer, Jürgen Freitag, Antje Merkau, Iris Nowak, and Claudia Heller. As always, Dieter Dettmar outdid himself in preparing superb polished thin sections from most difficult rocks. Jim Gardner probably has never received such an incomplete first draft of a manuscript for review 2 days before submission. We owe him a lot. The manuscript benefitted from critical comments by D.A. Swanson and R.V. Fisher. Our work was supported by grants from the Deutsche Forschungsgemeinschaft, grants Schm 250/40-1, 60-1, 2 and EC project MAS2-CT94-0083 (STEAM), which we gratefully acknowledge.

REFERENCES

Abdel Monem, A., Watkins, N.D., and Gast, P.W., 1971. Potassium-argon ages, volcanic stratigraphy, and geomagnetic polarity history of the Canary Islands: Lanzarote, Fuerteventura, Gran Canaria, and La Gomera. *Am. J. Sci.,* 271:490–521.

Binard, N., Hékinian, R., and Stoffers, P., 1992. Morphostructural study and type of volcanism of submarine volcanoes over the Pitcairn hot spot in the South Pacific. *Tectonophysics*, 206:245–264.

Cantagrel, J.-M., Cendrero, A., Fúster, J.-M., Ibarrola, E., and Jamond, C., 1984. K-Ar-chronology of the volcanic eruptions in the Canarian Archipelago: Island of La Gomera. *Bull. Volcanol.,* 47:597–609.

Cas, R.A.F., and Wright, J.V., 1987. *Volcanic Successions: Modern and Ancient:* London (Allen and Unwin).

————, 1991. Subaqueous pyroclastic flows and ignimbrites: An assessment. *Bull. Volcanol.*, 53:357–380.

Fisher, R.V., and Schmincke, H.-U., 1984. *Pyroclastic Rocks:* New York (Springer-Verlag).

Fiske, R.S. and Simkin, T., 1983. *Krakatau 1883:* Washington (Smithsonian Inst. Press).

Freundt, A., and Schmincke, H.-U., 1995. Eruption and emplacement of a basaltic welded ignimibrite during caldera formation on Gran Canaria. *Bull. Volcanol.*, 56:640–659.

Funck, T., and Schmincke, H.-U., in press. Growth and destruction of Gran Canaria deduced from seismic reflection and bathymetric data. *J. Geophys. Res*.

Kobberger, G., and Schmincke, H.-U., in press. Deformation history of rheomorphic ignimbrite D (Gran Canaria). *Bull. Volcanol.*

Moore, G.W., and Moore, J.G., 1988. Large scale bedforms in bolder graval produced by giant waves in Hawaii. *Spec. Pap.—Geol. Soc. Am.,* 229:101–109.

Orton, G.J., 1991. Emergence of subaqueous depositional environments in advance of a major ignimbrite eruption, Capel Curig volcanic formation, Ordovician, North Wales; an example of regional volcanotectonic uplift? *In* Cas, R.A.F., and Busby-Spera, Cathy, J. (Eds.), *Volcanoclastic Sedimentation.* Sediment. Geol., 74:251–286.

Schmincke, H.-U., 1969a. Ignimbrite sequence on Gran Canaria. *Bull. Volcanol.,* 33:1199–1219.

————, 1969b. Petrologie der phonolithischen bis rhyolithischen Vulkanite auf Gran Canaria, Kanarische Inseln [Habilitationsschrift]. Heidelberg, Ruprecht-Karl-Univ.

————, 1974. Volcanological aspects of peralkaline silicic welded ash-flow tuffs. *Bull. Volcanol.*, 38:594–636.

————, 1994. *Geological Field Guide: Gran Canaria* (7th ed.): Kiel, Germany (Pluto Press).

Schmincke, H.-U., and Swanson, D.A., 1967. Laminar viscous flowage structures in ash-flow tuffs from Gran Canaria, Canary Islands. *J. Geol.*, 75:641–664.

Schmincke, H.-U., and von Rad, U., 1979. Neogene evolution of Canary Island volcanism inferred from ash layers and volcaniclastic sandstones of DSDP Site 397 (Leg 47A). *In* von Rad, U., Ryan, W.B.F., et al., *Init. Repts. DSDP,* 47 (Pt. 1): Washington (U.S. Govt. Printing Office), 703–725.

Staudigel, H., and Schmincke, H.-U., 1984. The Pliocene seamount series of La Palma/Canary Islands. *J. Geophys. Res.*, 89:11195–11215.

Date of initial receipt: 5 August 1996
Date of acceptance: 22 January 1997
Ms 157SR-113

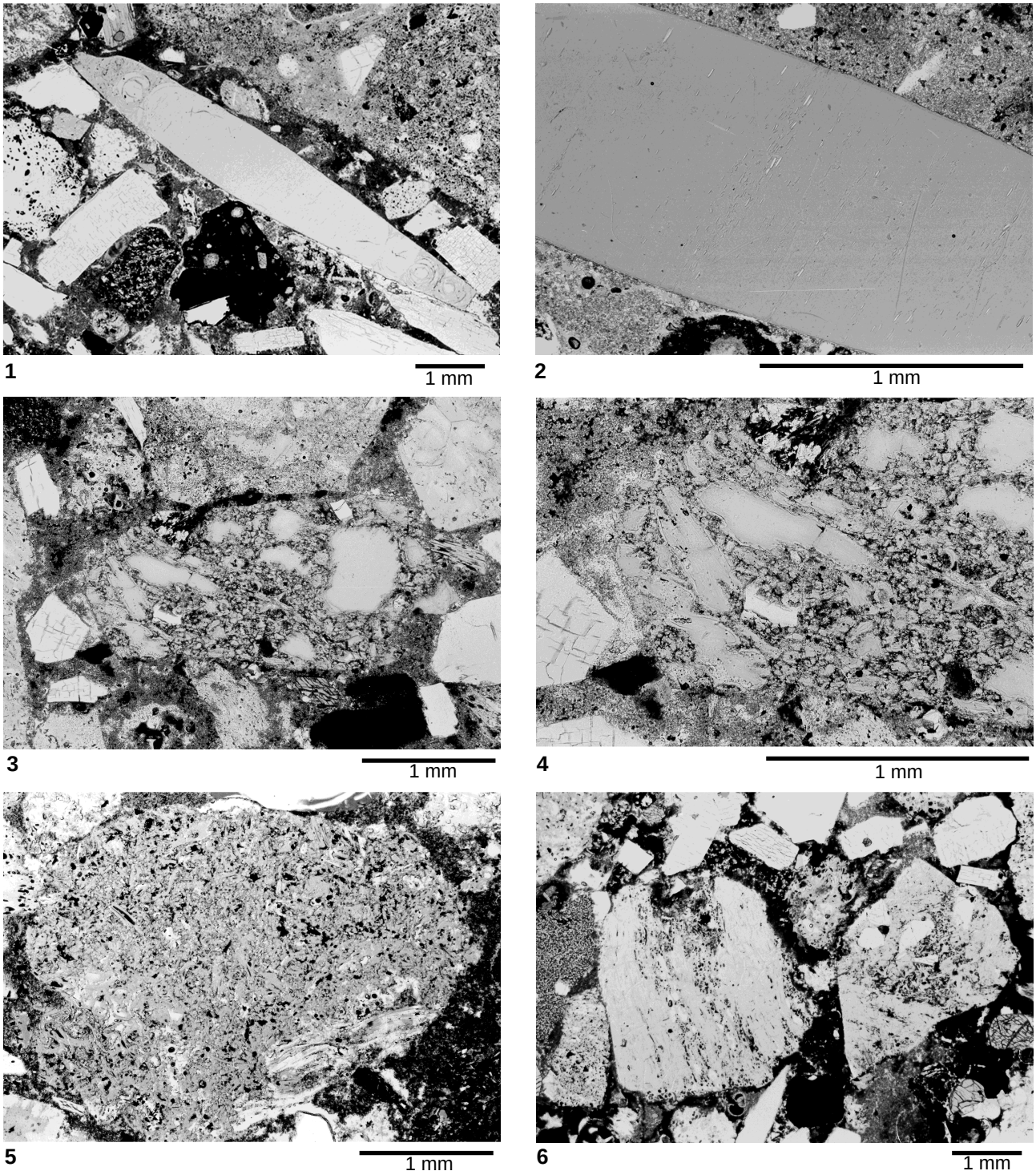

Plate 1. **1.** Splinter-like blocky rhyolitic glass shard (Sample 157-953C-64R-4, 62–74 cm). **2.** Detail of Figure 1 showing delicate traces of completely welded shards. **3.** Partially welded roundish rhyolitic glass shards with shard outlines still visible (Sample 157-953C-61R-3, 109–114 cm). **4.** Detail of Figure 3. **5.** Round shard of welded rhyolitic tuff showing differences in degree of welding within one shard (Sample 157-953C-61R-3, 99–105 cm). **6.** Two rhyolitic glass shards composed of layers of strongly and less strongly welded shards (Sample 157-953C-64 R-1, 62–74 cm).

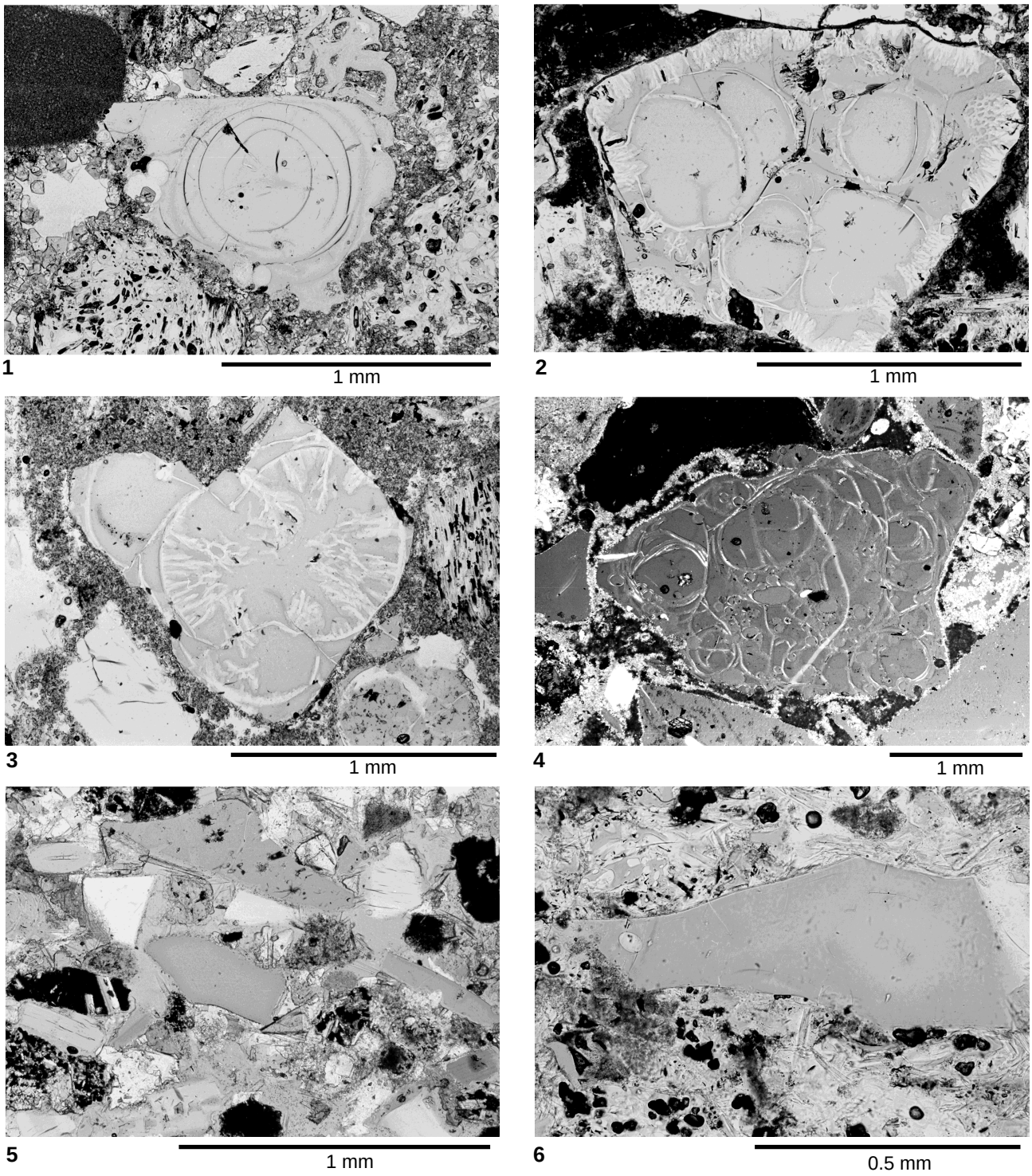

Plate 2. **1.** Blocky rhyolitic shard of completely welded tuff showing concentric perlitic alteration cracks (Sample 157-953C-64R-3, 72–75 cm). **2.** Large rhyolitic blocky shard of completely welded tuff showing four domains with concentric perlitic cracks and marginal bleached radial alteration channels (Sample 157-953C-61R–3, 109–114 cm). **3.** Blocky shard of completely welded rhyolitic tuff, partially altered (Sample 157-953C-61R-3, 99–105 cm). **4.** Blocky shard of completely welded rhyolitic tuff (Sample 157-953C-64R-4, 7–13 cm). **5.** Small angular shards in crystal-rich medium-grained rhyolitic tuff (Sample 157-953C-65R-1, 70–73 cm). **6.** Single, blocky, fresh shard of strongly welded rhyolitic tuff (Sample 157-953C-65R-2, 94–98 cm).

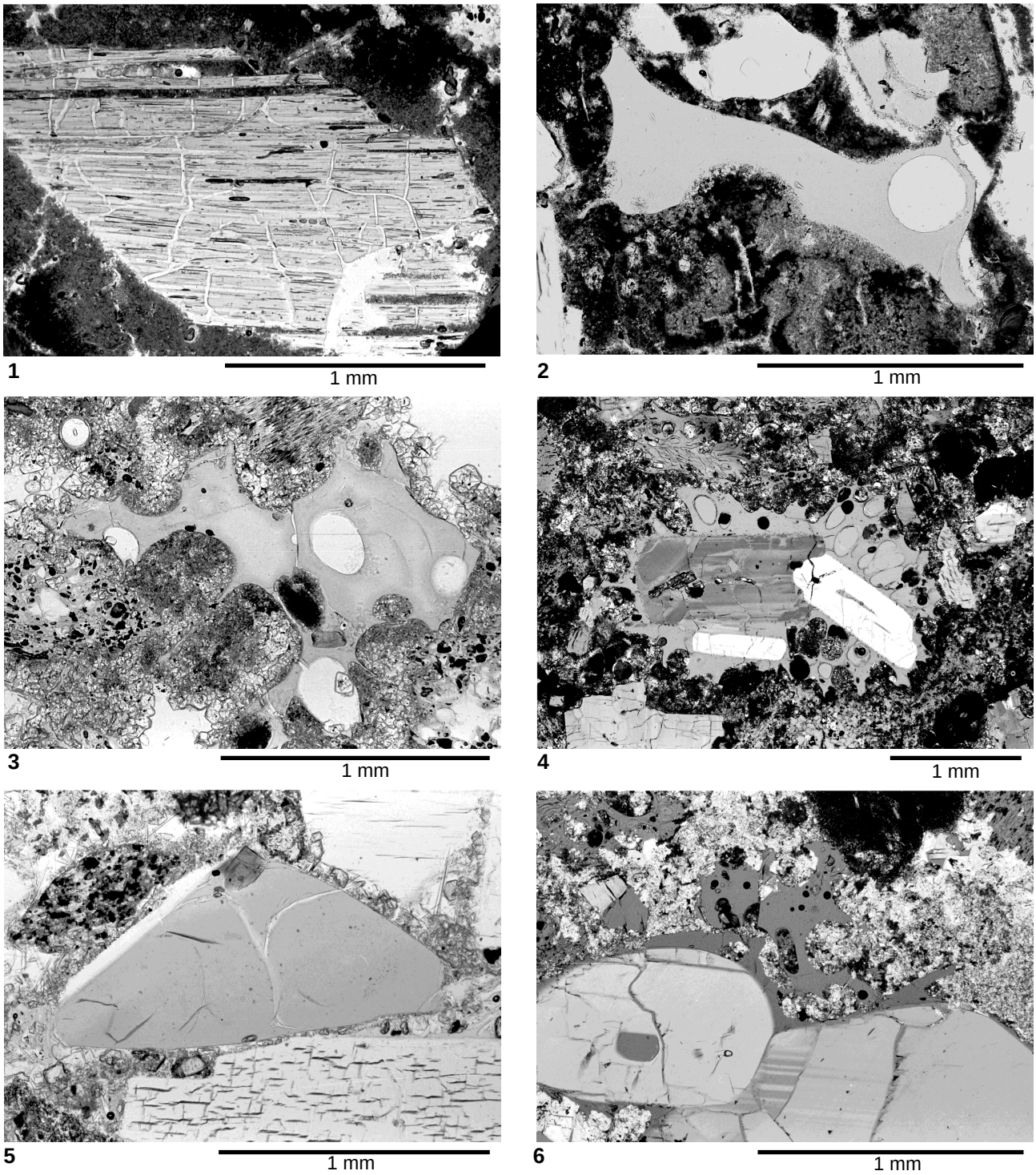

Plate 3. **1.** Fragment of strongly welded rhyolitic tuff with extremely stretched welded shards (Sample 157-953C-64R-1, 62–74 cm). **2.** Large single rhyolitic shard (Sample 157-953C-64R-4, 62–74 cm). **3.** Moderately vesiculated pantelleritic shard with thick glass septa (Sample 157-953C-64R-3, 72–75 cm). **4.** Anorthoclase crystal with thick lace-like glass rim (Sample 157-953C-68R-4, 56–60 cm). **5.** Feldspar fragment with glass rim (Sample 157-953C-62R-2, 0–4 cm). **6.** Thick glass shard and feldspar with glass rim and large melt inclusion (Sample 157-953C-68R-3, 60–66 cm).

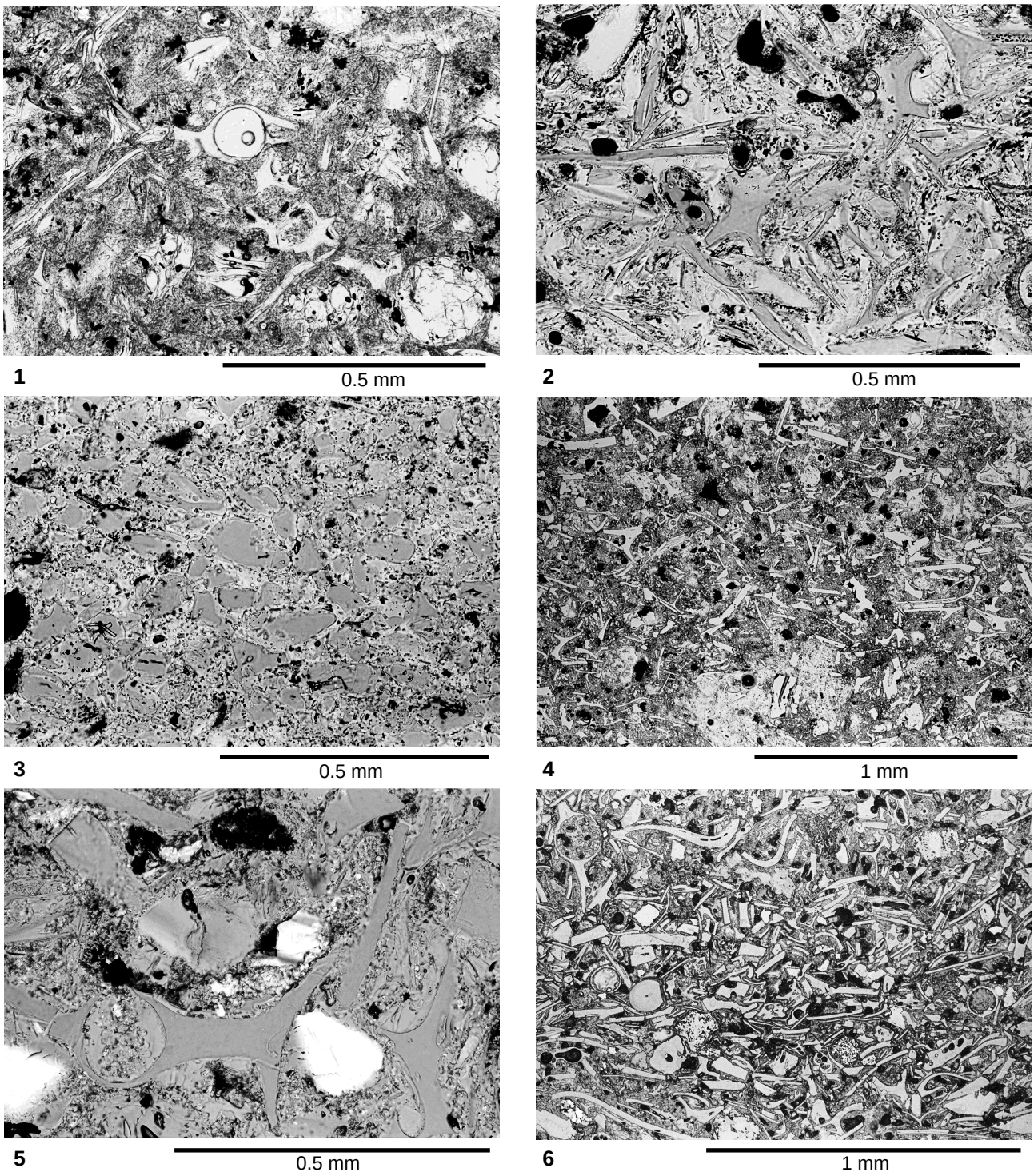

Plate 4. **1.** Vitric tuff consisting dominantly of rhyolitic bubble-wall shards with nannofossil matrix (Sample 157-953C-65R-6, 100–101 cm). **2.** Fresh bubble-wall glass shards in vitric tuffs (Sample 157-953C-67R-1, 148–150 cm). **3.** Spherical shards resulting from surface tension of hot pantelleritic ash particles (Sample 157-953C-61R-2, 139–141 cm). **4.** Vitric bubble-wall shard tuff with nannofossil matrix (Sample 157-953C-62R-4, 29–31 cm). **5.** Vitric tuff with bubble-wall shards (Sample 157-953C-68 R-1, 80–97 cm). **6.** Vitric tuff with bubble-wall shards (Sample 157-953C-67 R-3, 63–64 cm).

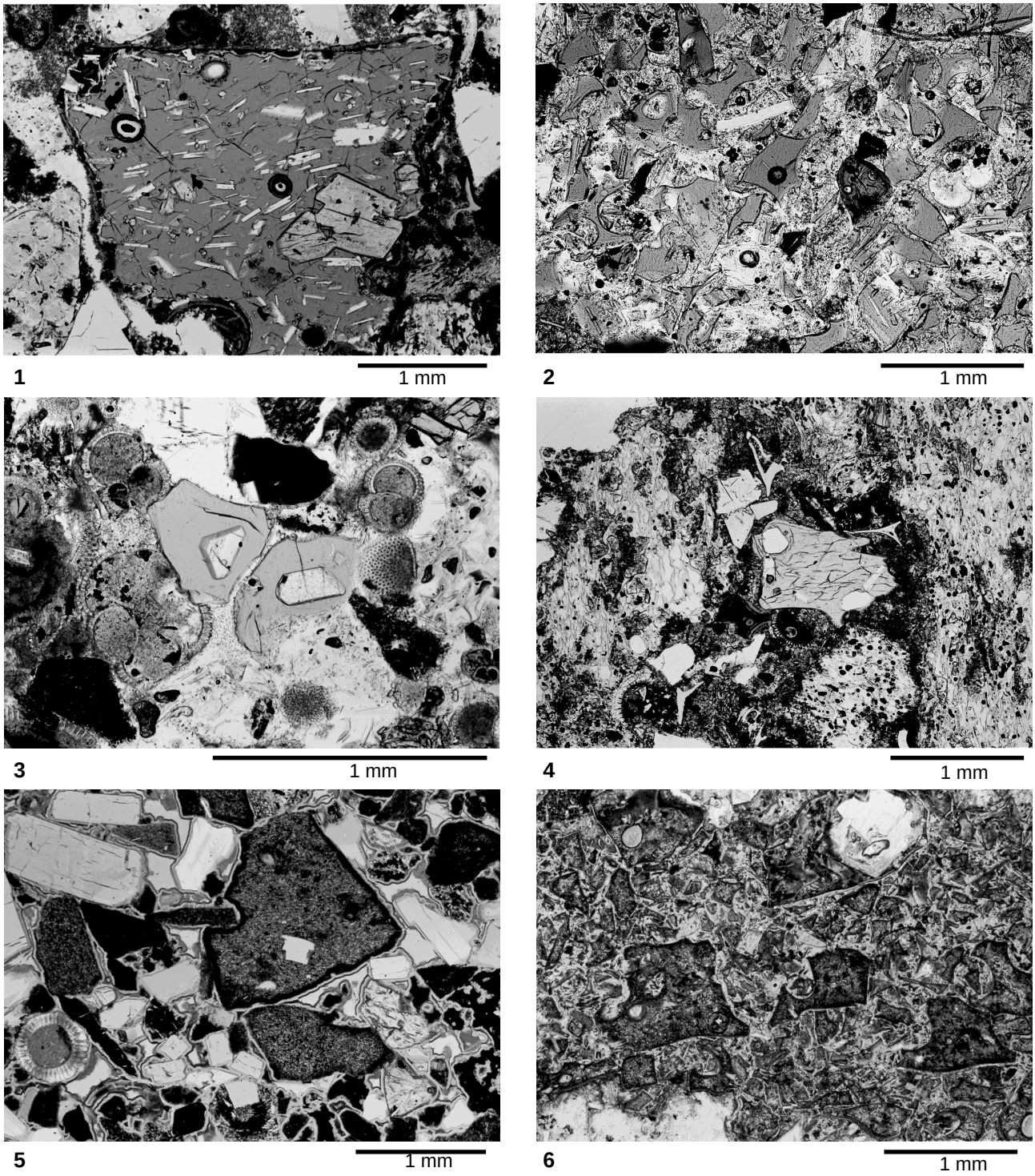

Plate 5. **1.** Large sideromelane shard with pyroxene, olivine phenocrysts, and plagioclase microlites and rhyolitic glass shards (Sample 157-953C-61R-3, 109–114 cm). **2.** Hyaloclastite consisting of moderately vesicular sideromelane shards, (Sample 157-956B-40R-1, 68–71 cm). **3.** Two sideromelane shards with small olivine microphenocrysts surrounded by *Globigerina*, vitric shards and rock fragments (Sample 157-953C-69R-1, 0–7 cm). **4.** Sideromelane shard with olivine microphenocrysts surrounded by rhyolitic pumice, rock fragment, bubble-wall shards and fragments of foraminifers (Sample 157-953C-68R-4, 56–60 cm). **5.** Quenched rhyolitic and slightly crystallized shards of ignimbrite P1, anorthoclase crystals and quenched tachylitic fragments from the basaltic part of P1 (Sample 157-953C-70R-3, 12–14 cm). **6.** Fragment of hyaloclastite tuff from the shield series incorporated into felsic volcaniclastic (Sample 157-953C-71R-4, 19–24 cm).